

**AD-A203 348**

**AAMRL-TR-88-038**



# **INVESTIGATION OF COMPOSITE MATERIALS FOR MANIKIN SKELETAL COMPONENTS, SMALL BUSINESS INNOVATION RESEARCH PHASE I FINAL REPORT**

**Caroline Van Ingen  
Joseph W. Coltman  
Simula Inc.  
10016 S 51st Street  
Phoenix AZ 85044**

**April 1988**

**Final report for September 1987 to May 1988**



**Approved for public release; distribution is unlimited.**

**89 2 7 07**

**HARRY G. ARMSTRONG AEROSPACE MEDICAL RESEARCH LABORATORY  
HUMAN SYSTEMS DIVISION  
AIR FORCE SYSTEMS COMMAND  
WRIGHT-PATTERSON AIR FORCE BASE, OHIO 45433-6573**

## NOTICES

When US Government drawings, specifications, or other data are used for any purpose other than a definitely related Government procurement operation, the Government thereby incurs no responsibility nor any obligation whatsoever, and the fact that the Government may have formulated, furnished, or in any way supplied the said drawings, specifications, or other data, is not to be regarded by implication or otherwise, as in any manner licensing the holder or any other person or corporation, or conveying any rights or permission to manufacture, use, or sell any patented invention that may in any way be related thereto.

Please do not request copies of this report from the Armstrong Aerospace Medical Research Laboratory. Additional copies may be purchased from:

National Technical Information Service  
5285 Port Royal Road  
Springfield, Virginia 22161

Federal Government agencies and their contractors registered with Defense Technical Information Center should direct requests for copies of this report to:

Defense Technical Information Center  
Cameron Station  
Alexandria, Virginia 22314

## TECHNICAL REVIEW AND APPROVAL

AAMRL-TR-88-038

This report has been reviewed by the Office of Public Affairs (PA) and is releasable to the National Technical Information Service (NTIS). At NTIS, it will be available to the general public, including foreign nations.

This technical report has been reviewed and is approved for publication.

**FOR THE COMMANDER**



HENNING E. VON GIERKE, Dr Ing

Director

Biodynamics and Bioengineering Division

Armstrong Aerospace Medical Research Laboratory

UNCLASSIFIED  
SECURITY CLASSIFICATION OF THIS PAGE

REPORT DOCUMENTATION PAGE				Form Approved OMB No. 0704-0188									
1a. REPORT SECURITY CLASSIFICATION <b>UNCLASSIFIED</b>			1b. RESTRICTIVE MARKINGS										
2a. SECURITY CLASSIFICATION AUTHORITY			3. DISTRIBUTION/AVAILABILITY OF REPORT Approved for public release; distribution is unlimited.										
2b. DECLASSIFICATION/DOWNGRADING SCHEDULE													
4. PERFORMING ORGANIZATION REPORT NUMBER(S) TR-88476			5. MONITORING ORGANIZATION REPORT NUMBER(S) AAMRL-TR-88-038										
6a. NAME OF PERFORMING ORGANIZATION Simula, Inc.		6b. OFFICE SYMBOL (If applicable)		7a. NAME OF MONITORING ORGANIZATION AAMRL/BBM									
6c. ADDRESS (City, State, and ZIP Code) 10016 S 51st Street Phoenix AZ 85044			7b. ADDRESS (City, State, and ZIP Code) Wright-Patterson AFB OH 45433-6573										
8a. NAME OF FUNDING/SPONSORING ORGANIZATION		8b. OFFICE SYMBOL (If applicable)		9. PROCUREMENT INSTRUMENT IDENTIFICATION NUMBER F33615-87-C-0544									
8c. ADDRESS (City, State, and ZIP Code)			10. SOURCE OF FUNDING NUMBERS										
			<table border="1"><tr><td>PROGRAM ELEMENT NO.</td><td>PROJECT NO</td><td>TASK NO</td><td>WORK UNIT ACCESSION NO</td></tr><tr><td>65502F</td><td>7231</td><td>36</td><td>06</td></tr></table>			PROGRAM ELEMENT NO.	PROJECT NO	TASK NO	WORK UNIT ACCESSION NO	65502F	7231	36	06
PROGRAM ELEMENT NO.	PROJECT NO	TASK NO	WORK UNIT ACCESSION NO										
65502F	7231	36	06										
11. TITLE (Include Security Classification) Investigation of Composite Materials for Manikin Skeletal Components - Phase I (Unclassified)													
12. PERSONAL AUTHOR(S) Caroline Van Ingen and Joseph W. Coltman													
13a. TYPE OF REPORT Final		13b. TIME COVERED FROM 870909 TO 880513		14. DATE OF REPORT (Year, Month, Day) 88 APR 28									
				15. PAGE COUNT 86									
16. SUPPLEMENTARY NOTATION Small Business Innovative Research (SBIR) Phase I contract													
17. COSATI CODES			18. SUBJECT TERMS (Continue on reverse if necessary and identify by block number)										
FIELD	GROUP	SUB-GROUP											
06	02		Manikin, Composite, femur										
06	07		MANNEQUINS, HUMAN FACTORS ENGINEERING										
19. ABSTRACT (Continue on reverse if necessary and identify by block number) The first part of this effort involved analyzing 50th percentile Hybrid III and human femoral bone properties for use in the design of a composite femur. Next, a prototype composite femur was fabricated. The prototype femur consisted of a laminated shaft of 22 ply graphite-epoxy and the knee joint was machined from a block of short fiberglass-reinforced thermoplastic. The hip joint assembly was composed of a titanium alloy neck, an aluminum bronze ball and a stainless steel retaining flange. A comprehensive testing study was conducted and the results indicated that the strength of the composite femur exceeded that of the Hybrid III and human femurs. The prototype composite femur weighed 3.9 lbs, which is much closer to the weight of the human femur which is approximately 2.0 lbs than the weight of the Hybrid III femur which is 12.5 lbs. The composite femur mass moments of inertia about the transverse axes ( $I_x$ and $I_y$ ) are 0.295 in-lb-sec <sup>2</sup> compared to 0.209 in-lb-sec <sup>2</sup> for the human femur and 0.96 in-lb-sec <sup>2</sup> for the Hybrid III. The moments of inertia for the composite femur are higher than that of													
20. DISTRIBUTION/AVAILABILITY OF ABSTRACT <input checked="" type="checkbox"/> UNCLASSIFIED/UNLIMITED <input type="checkbox"/> SAME AS RPT <input type="checkbox"/> DTIC USERS			21. ABSTRACT SECURITY CLASSIFICATION UNCLASSIFIED										
22a. NAME OF RESPONSIBLE INDIVIDUAL ROY RASMUSSEN			22b. TELEPHONE (Include Area Code) (513) 255-3667		22c. OFFICE SYMBOL AAMRL/BBM								

DD Form 1473, JUN 86

Previous editions are obsolete

SECURITY CLASSIFICATION OF THIS PAGE  
UNCLASSIFIED

19. ABSTRACT (Continued)

the human as a result of weight concentration at the ends of the femur to allow for Hybrid III dummy joint compatibility. The composite femur, however, allows a greater proportion of the mass to be contributed by the flesh covering, resulting in a better approximation of the overall segment mass moments of inertia ( $I_x$ ,  $I_y$  and  $I_z$ ). This effort verified that the use of composite materials in manikin skeletal components is feasible.

## PROJECT SUMMARY

The objective of this research effort was to determine the feasibility of using composite materials in manikin skeletal components. The skeletal components of current manikins are constructed out of various metals, resulting in excessively stiff and heavy components that lack biofidelic response characteristics. Phase I was designed to develop a composite manikin femur that could be tested to verify the feasibility of using composites as structural components in the remaining skeletal system.

Human femoral properties were analyzed and composite materials researched to design a manikin femur that exhibited the weight and mass moments of inertia of a human femur and a strength that exceeded the Hybrid III femur. A prototype composite femur was fabricated and statically tested, affirming the feasibility of using composite materials in manikin skeletal components.

A proposed Phase II program will continue the development effort with composites for the limbs of a test manikin. The approach used to design and fabricate the composite femur in Phase I will be used. In addition to skeletal segments for arms, legs, feet, and hands, flesh segments for these components will be developed. Commercialization of composite manikin segments will take place during Phase III.

Based on the success of Phase I, a recommendation is made to continue the development effort with composites for each skeletal component to achieve a completely biofidelic manikin.



Accession For	
NTIS GRA&I	<input checked="checked" type="checkbox"/>
DTIC TAB	<input type="checkbox"/>
Unannounced	<input type="checkbox"/>
Justification	
By	
Distribution/	
Availability Codes	
Dist	
A-1	

### ACKNOWLEDGMENT

This final report describes work conducted under a Phase I Small Business Innovation Research (SBIR) program entitled "Investigation of Composite Materials for Manikin Skeletal Components." Funding for this program was supplied by the Department of the Air Force Systems Command, Aeronautical Systems Division, under Contract No. F33615-87-C-0544. This contract was administered by the Armstrong Aerospace Medical Research Laboratory (AAMRL), Wright-Patterson Air Force Base, Ohio.

Dr. Ints Kaleps provided technical direction as the Contracting Officer's Technical Representative for AAMRL.

## TABLE OF CONTENTS

	<u>Page</u>
1.0 INTRODUCTION . . . . .	1
2.0 IDENTIFICATION AND SIGNIFICANCE OF THE PROBLEM . . . . .	2
3.0 PHASE I TECHNICAL OBJECTIVES . . . . .	5
4.0 ANALYSIS OF HYBRID III AND HUMAN FEMORAL PROPERTIES. . . . .	6
4.1 REVIEW OF HYBRID III FEMUR. . . . .	6
4.2 REVIEW OF HUMAN FEMUR . . . . .	6
5.0 ADVANCED COMPOSITE FEMUR DESIGN AND FABRICATION. . . . .	9
5.1 DESIGN FACTORS. . . . .	9
5.1.1 Design Parameters. . . . .	9
5.1.2 Design Loads . . . . .	10
5.2 COMPONENT FEATURES. . . . .	15
5.2.1 Overall Characteristics. . . . .	15
5.2.2 Detailed Component Design. . . . .	17
5.2.3 Weight and Center of Gravity . . . . .	27
5.2.4 Recommended Flesh Design . . . . .	27
6.0 MECHANICAL TESTING . . . . .	35
6.1 PURPOSE . . . . .	35
6.2 TEST PLAN . . . . .	35
6.3 TEST RESULTS. . . . .	37
6.3.1 Test 1 - Torsion . . . . .	37
6.3.2 Test 2 - Compression . . . . .	37
6.3.3 Test 3 - Combined Lateral Bending/Torsion. . . . .	37
6.3.4 Test 4 - Lateral Bend Test . . . . .	42
6.3.5 Test 5 - Lateral Test of Titanium Neck . . . . .	42
7.0 FEASIBILITY ANALYSIS . . . . .	43
7.1 FEASIBILITY OF COMPOSITE MATERIAL . . . . .	43
7.2 FEASIBILITY OF COMPOSITE FEMUR. . . . .	43
7.3 FEASIBILITY OF REMAINING SKELETAL COMPONENTS. . . . .	45

## TABLE OF CONTENTS (CONTD)

	<u>Page</u>
8.0 CONCLUSIONS. . . . .	46
9.0 RECOMMENDATIONS. . . . .	47
10.0 REFERENCES . . . . .	48
APPENDIX A - HUMAN BONE AND FEMUR PROPERTIES. . . . .	A-1
APPENDIX B - CALCULATIONS OF COMPOSITE FEMUR LOADS. . . . .	B-1
APPENDIX C - LAMINATED SHAFT STRAINS, STRESSES, AND SAFETY FACTOR FOR THE LOADS SHOWN IN FIGURE 6. . . . .	C-1
APPENDIX D - CALCULATIONS OF STRESS IN THE KNEE FITTING . . . . .	D-1
APPENDIX E - CALCULATION OF ULTIMATE STRENGTH OF YELLOW BRASS NECK OF EXISTING HYBRID III FEMUR . . . . .	E-1



## LIST OF ILLUSTRATIONS

<u>Figure</u>		<u>Page</u>
1	Comparison between human femur and Hybrid III femur. . . . .	4
2	Structural schematic of Hybrid III upper and lower leg (using aircraft coordinate system) . . . . .	11
3	Design loading conditions for Hybrid III femur . . . . .	12
4	Advanced composite femur design. . . . .	16
5	Advanced composite femur prototype . . . . .	17
6	Comparison of relative position ( $\delta$ ) between center of hip joint ball and axis of shaft for each femur. . . . .	18
7	Forces acting on laminated shaft for side-facing seat (critical loading Case 2B.) . . . . .	20
8	Laminated shaft assembly . . . . .	21
9	Critical loading of advanced composite knee joint fitting (lateral load - side-facing troop seat). . . . .	22
10	Advanced composite knee joint fitting design . . . . .	23
11	Advanced composite knee joint fitting prototype. . . . .	24
12	Subcomponents of the hip joint assembly. . . . .	25
13	Advanced composite hip joint assembly. . . . .	26
14	Required location, weight, and moments of inertia of advanced composite femur . . . . .	30
15	Design of recommended flesh covering . . . . .	32
16	Composite disc for retention of flesh covering.. . . .	33
17	Flesh covering of lower leg of ADAM. . . . .	34
18	Test 1 - Torsion . . . . .	36
19	Test 2 - Compression . . . . .	37
20	Test 3 - Bending . . . . .	38
21	Test 4 - Combined bending/tension. . . . .	39
22	Test 5 - Lateral bend test of titanium neck. . . . .	40
23	Posttest view - static test, torsion . . . . .	41

## LIST OF ILLUSTRATIONS

<u>Figure</u>		<u>Page</u>
24	Static testing, lateral bend test of titanium neck. . . . .	42
25	Comparison of properties for materials used in advanced composite femur . . . . .	44

## LIST OF TABLES

<u>Table</u>		<u>Page</u>
1	Hybrid III femur components and weights. . . . .	7
2	Mass and mass moments of inertia of human and Hybrid III femurs . . . . .	8
3	Crash pulses and magnitudes (from MIL-S-58095A). . . . .	10
4	Summary of design loads for Hybrid III femur. . . . .	13
5	Loading case table - Hybrid III femur. . . . .	14
6	Properties of ULTEM 2000 . . . . .	21
7	Comparative strengths of cast yellow brass (SAE CA863) and Titanium Ti-6Al-4V . . . . .	24
8	Weights of advanced composite femur components . . . . .	28
9	Upper leg and femoral mass for human, Hybrid III and composite prototype. . . . .	29
10	Upper leg and femoral mass moments of inertia. . . . .	29
11	Potential flesh cover materials. . . . .	31
12	Final static test results on composite femur . . . . .	41

## 1.0 INTRODUCTION

The intent of the Phase I effort was to demonstrate the feasibility of using composite materials in manikin skeletal components. The skeletal components of manikins are currently constructed of various metals, resulting in excessively stiff and heavy components that do not provide biofidelic (human-like) response characteristics. The advantages of using composite materials is two-fold: to produce more human-like characteristics, such as mass, mass moments of inertia and dynamic response; and to maintain the degree of strength required to sustain the high loads of dynamic testing. The femur (upper leg bone) was selected in Phase I as a representative skeletal component.

With the femur chosen as the test component, the program focused on several major objectives. First, the Hybrid III manikin and human femoral bone properties were analyzed and used to design an advanced femur concept. Next, a prototype manikin femur was fabricated and subjected to static testing. The combined objectives provided a comprehensive study to verify the prototype design and the feasibility of using composites in manikin skeletal components.

## 2.0 IDENTIFICATION AND SIGNIFICANCE OF THE PROBLEM

Anthropomorphic manikins were first developed after World War II when newly developed ejection seats for high performance aircraft needed to be tested. The need for human surrogates still exists, along with an increasing demand that these manikins be more representative of humans.

While the Hybrid III anthropomorphic test manikin is considered state of the art and an improvement over the former "standard" manikin, it is still far from the "ultimate" test manikin (Reference 1). However, development of a manikin with improved dynamic response is well underway with the Advanced Dynamic Anthropomorphic Manikin (ADAM) program (Reference 2). Nevertheless, modern manikins such as the Hybrid III and ADAM are comprised of a skeleton of metal "bones" to provide the structural strength required to withstand the high accelerations and loads experienced during dynamic testing. These excessively stiff and heavy metallic structures constrain achievement of proper segment inertial distribution and deformation properties, especially in the load-transmitting members of the skeleton, such as the tibia, femur, pelvis, and spine.

The total mass of the manikin is concentrated in these skeletal components and in long segments it is not as well distributed along the radial axis as along the longitudinal axis. Consequently, the moment of inertia is distorted along the longitudinal axis.

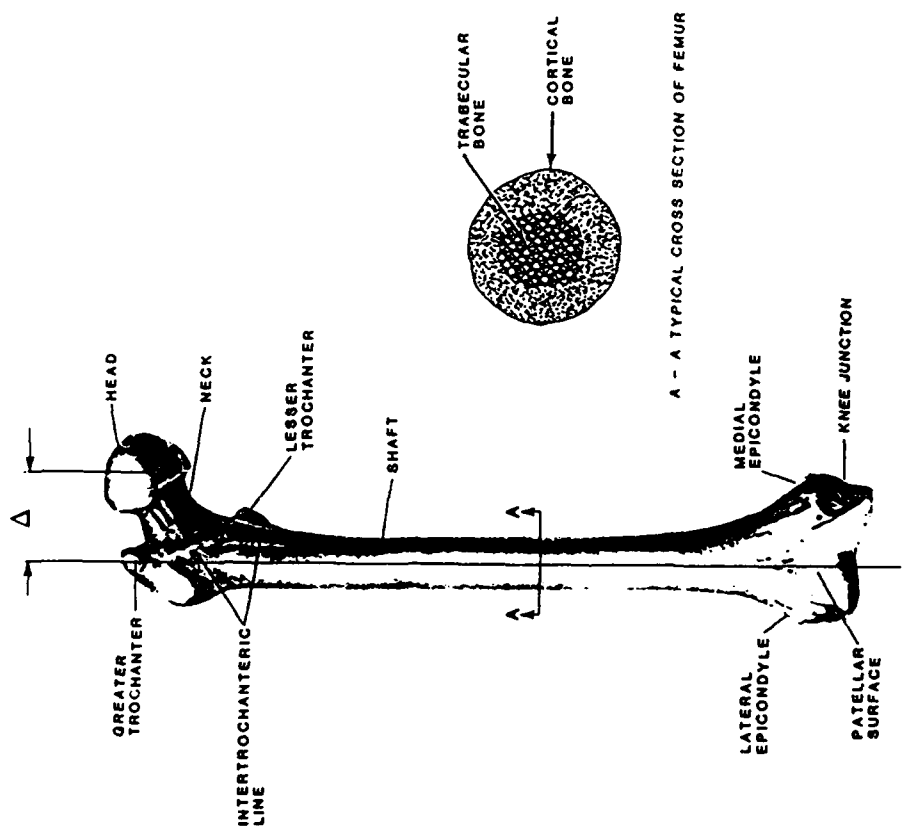
In addition to bearing an unrealistically high percentage of the total body weight, metallic components in the manikin do not transmit loads representatively. For instance, experiments involving impacts of the lower limb, which is pin-jointed at the knee, resulted in excessively high peak forces in the femur of the Hybrid III (Reference 3). As a result of knee impact forces, load transmission through the femur also causes excessively high loads in the pelvis. It has been shown that as a result of these loads, the manikin femur has a tendency to break in the upper portion of its length (Reference 4).

Another segment that lacks biofidelity in the Hybrid III is the spinal column, which fails to fully accommodate vertical loading. The lumbar spine is a uniquely composed polyacrylate elastomeric member with two steel cables running the length of its lordotic curvature. The thoracic spine, on the other hand, is composed of welded steel. The interface between the thoracic spine and the lumbar spine does not accommodate for this difference in material properties, causing the load-deformation and load-transmitting properties between these two components to be distorted.

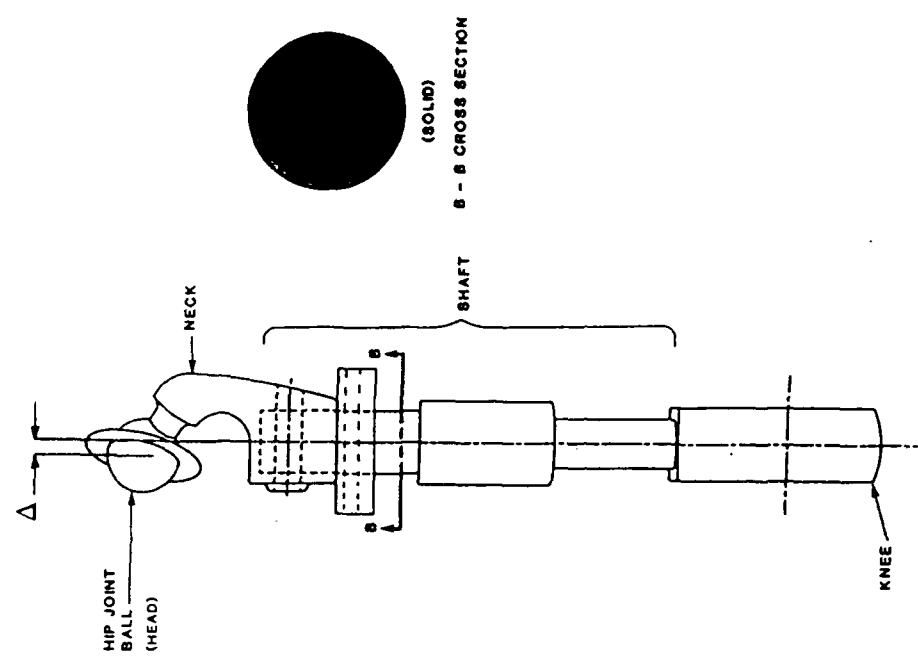
The connecting of skeletal components of different materials, such as the thoracic and lumbar spines, is the cause of poor biofidelity in the total manikin. Poor coupling also exists between the "bony" and "fleshy" components of a segment. In the Hybrid III, for example, the integration of a light, foam thigh with a dense, metallic femur, does not lend itself to proper load transmission.

As an alternative to metals, composite materials have a higher strength-to-weight ratio and have more bonelike deformation properties than the currently used metal parts, thereby offering a significant improvement over the current characteristics of both the Hybrid III and the ADAM. For this SBIR investigation, the Hybrid III was used as a baseline for the development of a composite manikin, and the results of the ongoing ADAM program were addressed. Figure 1 compares the human femur with the femur currently used in the Hybrid III. An anatomical difference is shown in the figure by the relative distance ( $\Delta$ ) between the hip joint ball center and the longitudinal axis of each shaft. Cross sections of each femur further illustrate the poor resemblance between them. A difference in mass between the femurs also exists: the Hybrid III femur weighs 12.5 lb while the human femur weighs only 2 lb. The femur was selected in this program as a representation of all the skeletal components for determining the feasibility of using composite materials in manikin skeletons.

It should be noted, however, that simply changing the skeletal components will not correct all the problems in the manikin, but rather will begin a chain of modifications to satisfy the requirements for a completely bio-fidelic response.



a. HUMAN FEMUR WITH TYPICAL CROSS-SECTION



b. HYBRID III FEMUR WITH CROSS-SECTION

NOTE

$\Delta$  = RELATIVE DISTANCE BETWEEN HIP JOINT BALL CENTER AND LONGITUDINAL AXIS OF SHAFT

FIGURE 1. COMPARISON BETWEEN HUMAN FEMUR AND HYBRID III FEMUR.

### 3.0 PHASE I TECHNICAL OBJECTIVES

The primary goal of the Phase I effort was to develop an advanced concept of the Hybrid III manikin femur using composite materials to reduce its weight and improve its inertial properties. The new femur was to respond more like that of a human but still exhibit the high strength found in existing manikins. The Phase I results, therefore, would demonstrate the overall feasibility of using composite materials to achieve more biofidelic characteristics in the remaining skeletal components of anthropomorphic manikins. This objective would be demonstrated in Phases II and III of this program.

To reach the Phase I goal, the following four technical objectives had to be met:

- Analyze the Hybrid III manikin and human femoral bone properties through a literature search and observation of existing manikin parts and drawings
- Design an advanced concept of the femur using the Hybrid III femur as a baseline concept with given boundary conditions
- Fabricate a prototype manikin femur for demonstration and testing purposes
- Conduct static testing of the prototype to verify its design and to determine the feasibility of using composites in a manikin skeletal component.

Sections 4.0 through 7.0 elaborate on how these technical objectives were satisfied.



#### **4.0 ANALYSIS OF HYBRID III AND HUMAN FEMORAL PROPERTIES**

The properties of a representative 50th-percentile male aviator's femur were used to design a composite manikin femur. The 50th-percentile Hybrid III manikin femur, which, for purposes of this program included the knee, was used as a baseline for concept demonstration.

An analysis of the Hybrid III and human femoral properties was initially conducted through a study of the literature. The Hybrid III femur was also analyzed by observation of an existing Hybrid III femur and corresponding drawings. The human femur was further analyzed through an experimental characterization study.

##### **4.1 REVIEW OF HYBRID III FEMUR**

The upper portion of the Hybrid III femur (the hip joint assembly) consists of an aluminum bronze hip joint ball, 1.75 in. in diameter, and a yellow brass neck, 0.8 in. in diameter, connected by a hole bored in the ball. A ring flange made of aluminum bronze is used to retain the hip joint ball in the pelvic socket of the manikin. The total weight of this hip joint assembly is 3.2 lb. Connected to the neck, the upper leg is made from 1018 steel and weighs 5.2 lb. Extending from the upper leg is a second shaft, also made of 1018 steel, that weighs 1.4 lb. This second shaft inserts into the knee and is interchangeable with an aluminum load cell having the same dimensions. Weighing 2.6 lb, the knee is cast from aluminum and provides the rotation and stops for lower leg movement. The knee is connected to the lower leg with the following components: a delrin bushing and washer; a 303 stainless steel knee adapter assembly and nut; a cast thermoset urethane washer; and two 1018 steel knee lugs. A knee insert made of molded 45-durometer butyl rubber and an outer vinyl covering complete the knee.

The Navy observed that the Hybrid III leg assembly was unable to sustain the given loads when subjected to high speed ejection seat tests (Reference 4). The high moments developed in the hip joints due to the excessive flailing of the limbs caused them to break. Confirming this report, Simula examined a Hybrid III femur supplied by the Air Force and found that the aluminum bronze neck of the hip joint assembly had a severe change in shaft angle, primarily from sustaining the high applied loads. Similarly, the retaining ring (also made of the soft aluminum bronze) exhibited a notable dent in its shape caused by the force of the neck pressing against it.

In addition to the poor strength of the hip joint assembly of the Hybrid III manikin femur, the upper leg responds in a less biofidelic manner due to the excessive mass of the femur and the concentration of this mass at the ends of the bone. Table 1 lists the components of the Hybrid III femur and the weight of each. The total weight of the Hybrid III femur is 12.5 lb, which is at least 10 lb more than the weight of the human femur.

##### **4.2 REVIEW OF HUMAN FEMUR**

The properties of the human femur that are essential in designing a composite femur include weight, mass moments of inertia, and center of gravity. Properties that are less significant to the purpose of this program, but which are

TABLE 1. HYBRID III FEMUR COMPONENTS  
AND WEIGHTS

Part	Weight (lb)
Hip joint ball	0.580
Neck	.625
Upper shaft	5.201
Lower shaft	1.398
Knee	<u>2.692</u>
Total Weight	12.49

still of notable interest, include the mechanical properties of bone such as ultimate tensile strength, compressive strength, bending strength, torsional strength, modulus of elasticity, and density. Appendix A lists these properties for human compact bone, which is the most typical bone of the femur. Mechanical properties of the human femur as a component are also listed in Appendix A and served as a comparison to the Hybrid III and composite femurs.

Typically, for a human femur the elastic modulus is approximately 2,600 ksi (18 GPa), ultimate tensile strength is 17.8 ksi (123 MPa), and density is 0.065 lb/in.<sup>3</sup> (1.8 gm/cm<sup>3</sup>). The advanced composite femur was designed to meet or exceed the strengths of the existing Hybrid III manikin femur, which is designed to exceed the human strength properties shown in Appendix A. Exceeding human strength properties allows a manikin to be repeatedly tested without the failure that would normally exist in a human skeleton under similar loads.

In addition to the femoral properties found in the literature, an experimental analysis was conducted on a cadaveric femur to determine its load deflection properties, mass moments of inertia and center of gravity. Representative of a 50th-percentile male femur, the experimental femur weighed 1.9 lb and had an overall length of 18.5 in., a hip-joint ball diameter of 1.87 in., and a neck/shaft angle of 140 degrees. It was decided, after consultation with the Air Force, that simulating the load deflection properties of the human femur was of secondary importance. Instead, the inertial properties of the femur and flesh covering were the necessary design parameters. Consequently, the mass and mass moments of inertia of the femur were deemed necessary to achieve an overall human representation of the upper leg. Appendix A includes the experimental load-deflection measurements of the human femur, while Table 2 lists the mass and mass moments of inertia of the human and Hybrid III femurs. The difference in mass properties shown in Table 2 illustrates the distortion between the human and Hybrid III skeletal properties.

---

TABLE 2. MASS AND MASS MOMENTS OF INERTIA  
OF HUMAN AND HYBRID III FEMURS

---

Type of Femur	Mass (m) (lb)	Mass Moment of Inertia ( $I_x \approx I_y$ ) (in-lb-sec <sup>2</sup> )
Human	1.9	0.21
Hybrid III	12.5	0.96

---

## 5.0 ADVANCED COMPOSITE FEMUR DESIGN AND FABRICATION

### 5.1 DESIGN FACTORS

#### 5.1.1 Design Parameters

The design parameters for the advanced composite femur included the following (in order of decreasing importance):

- High strength-to-weight ratio
- Biofidelic mass and inertial properties
- Joint compatibility between femur and Hybrid III
- Ability to disassemble
- Biofidelic deformation properties.

**5.1.1.1 High Strength-to-Weight Ratio.** It was most important that the advanced composite femur be designed so that its weight would be more representative of the human femur weight of approximately 2.0 lb than of the Hybrid III femur weight of 12.5 lb. In addition, its strength needed to meet or exceed that of the Hybrid III femur. Due to the high strength-to-weight ratio exhibited by composites, these materials were ideal candidates to meet this design parameter.

**5.1.1.2 Biofidelic Mass and Inertial Properties.** The femur was designed so that, in conjunction with a flesh covering, it would simulate the mass and mass moments of inertia of the combined human femur and flesh.

**5.1.1.3 Joint Compatibility Between Femur and Hybrid III.** In order for the advanced composite femur to be properly evaluated, it needed to fit into the existing Hybrid III manikin for field testing. Therefore, the design was limited to the existing end fittings at the knee and hip joint of the Hybrid III. It is important to note that the potential to improve the design exists if the requirement for the femur to fit into the Hybrid III manikin is eliminated.

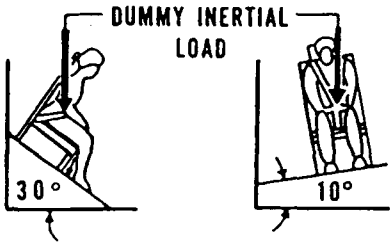
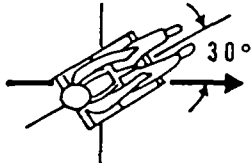
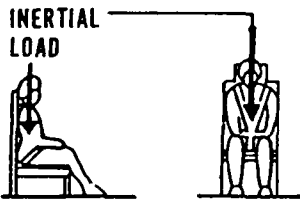
**5.1.1.4 Ability to Disassemble.** The femur was designed with a disassembly feature so that during testing, the replacement of any section that failed would be possible. This is an important feature of the design phase since it reduces the expense of replacing an entire component. It should be noted, however, that the disassembly feature hinders design optimization and will probably be eliminated from final versions.

**5.1.1.5 Biofidelic Deformation Properties.** Reproducing the strength and bending characteristics of the human bone in the composite femur, although desirable, is not necessary in order to achieve a biofidelic, kinematic response from the total upper leg, femur and flesh combined.

### 5.1.2 Design Loads

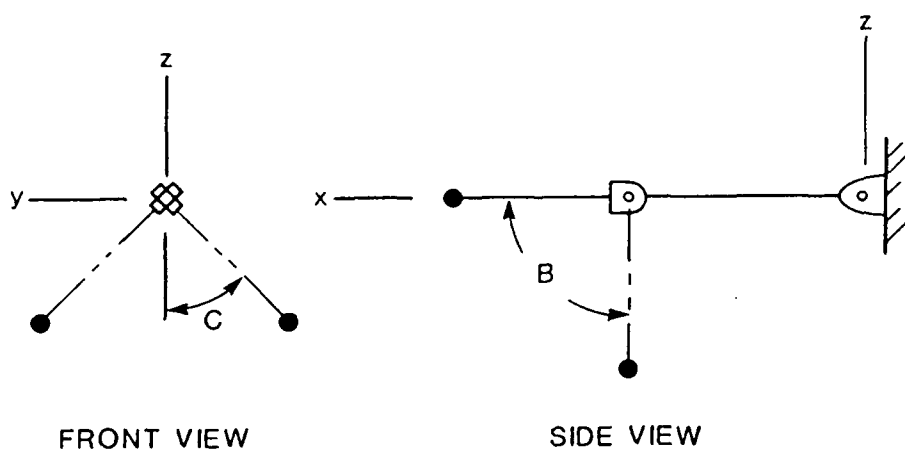
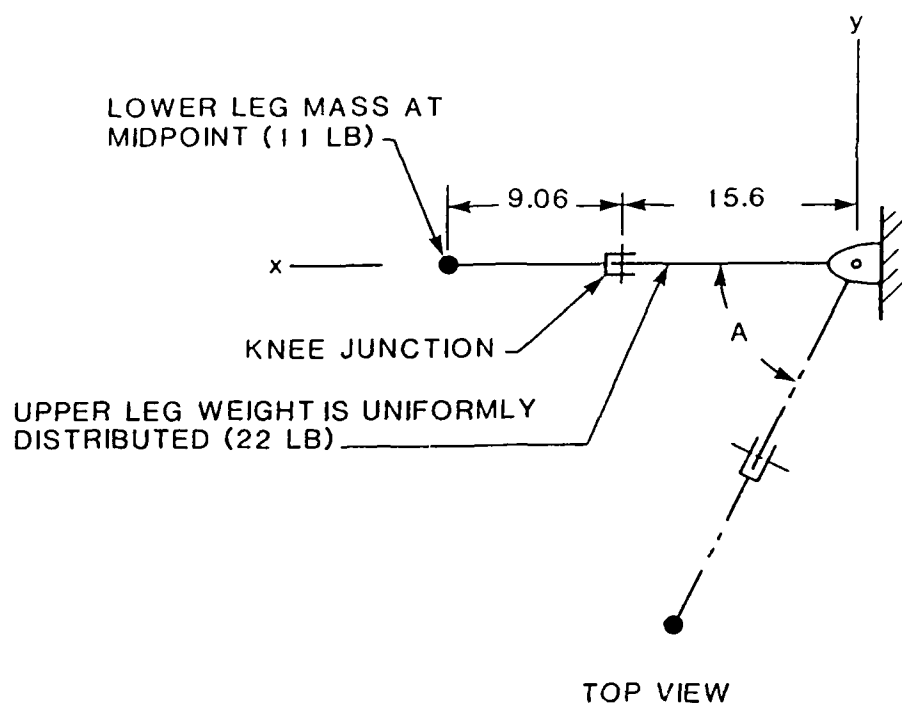
Structural design criteria for the advanced composite femur were based on inertial loads expected during dynamic tests involving anthropomorphic manikins. The most common of these dynamic tests involve simulated crash testing and aircraft ejection seat operations. Predicted maximum forces were based on the dynamic test requirements for crash testing specified in Table 3 (Reference 5). The lateral force component from crash test 2 was believed to be representative of wind blast forces experienced with ejection seats. Similarly, the vertical landing from crash tests 3 and 4 are equal to, or greater than, the vertical forces experienced in ejection seats.

TABLE 3. CRASH PULSES AND MAGNITUDES (FROM MIL-S-58095A)

TEST	CONFIGURATION	PARAMETER	LIMITS
1		$t_1$ SEC $t_2$ SEC G MIN G MAX $\Delta V$ MIN, FT/SEC (M/SEC)	0.043 0.061 46 51 50 (15.2)
2		$t_1$ SEC $t_2$ SEC G MIN G MAX $\Delta V$ MIN, FT/SEC (M/SEC)	0.066 0.100 28 33 50 (15.2)
3 & 4		$t_1$ SEC $t_2$ SEC G MIN G MAX $\Delta V$ MIN, FT/SEC (M/SEC)	0.036 0.051 46 51 42 (12.8)

88 02017 02

The Hybrid III leg was represented by the mechanical schematic shown in Figure 2. Several load cases were examined to determine the critical loading for the composite femur. The loading conditions used for the design and analysis are shown in Figure 3 and tabulated in Table 4. The externally applied forces shown in Table 4 were used to calculate the maximum forces and moments acting on the femur, which are tabulated in Table 5. The detailed calculations are presented in Appendix B.



NOTE (FROM REFERENCE 6)

$A = \pm 55^\circ$

$B = 0 \text{ TO } 90^\circ$

$C = \pm 45^\circ$

FIGURE 2. STRUCTURAL SCHEMATIC OF HYBRID III UPPER AND LOWER LEG (USING AIRCRAFT COORDINATE SYSTEM).

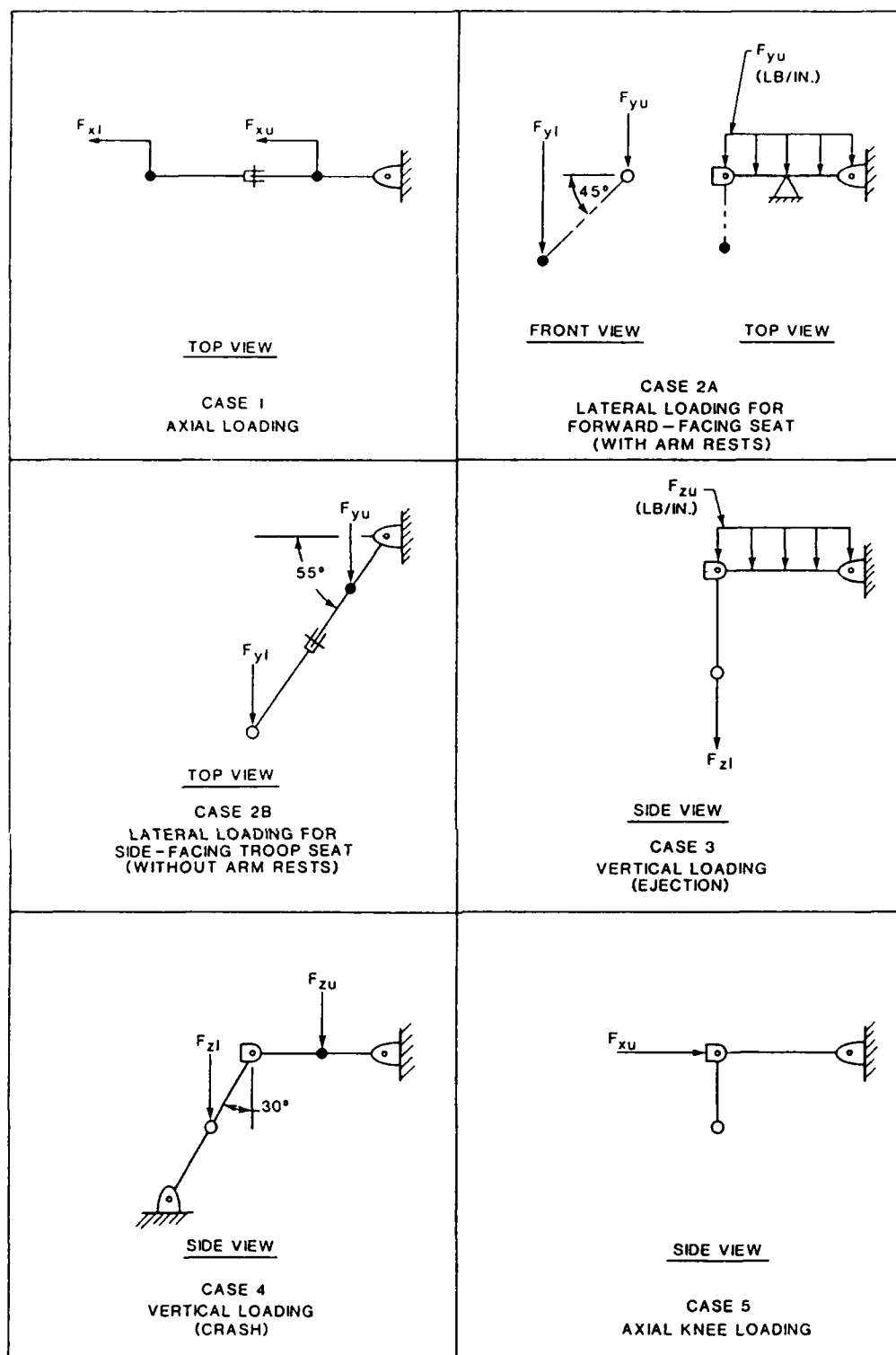


FIGURE 3. DESIGN LOADING CONDITIONS FOR HYBRID III FEMUR.

TABLE 4. SUMMARY OF DESIGN LOADS FOR HYBRID III FEMUR<sup>(1)</sup>

Load Case	Test No. (2)	Lower Leg (l)			Upper Leg (u)		
		$F_{xl}$	$F_{yl}$	$F_{zl}$	$F_{xu}$	$F_{yu}$	$F_{zu}$
1	2	944 lb	0	0	1,887 lb	-	-
2A	2	0	545 lb	0	0	69.8 lb/in. <sup>(4)</sup>	0
2B	2	0	944 lb	0	0	1,887 lb	0
3	(3)	0	0	759 lb	0	0	97.3 lb/in. <sup>(4)</sup>
4	3&4	0	0	1,683 lb	0	0	3,366 lb
5	N/A	0	0	0	8,640 lb	0	0

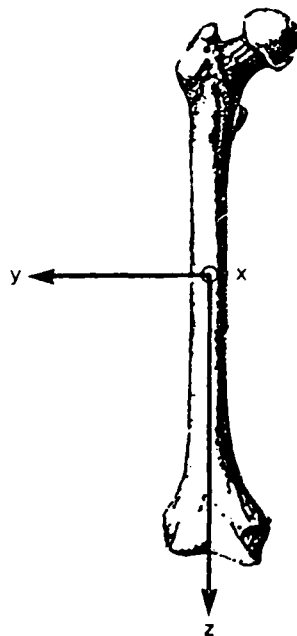
NOTES

1. See Figure 3 for location of applied forces. The forces tabulated include a dynamic factor of 2.0, and an ultimate load factor of 1.5. These factors have been applied to the G limits from MIL-S-58095A (as shown in Table 3).
2. From MIL-S-58095A, Table III.
3. MIL-S-58095A specifies a maximum occupant vertical acceleration of 23 G. which is consistent with vertical ejection accelerations.
4. Forces represent a distributed load over length of femur.



TABLE 5.      LOADING CASE TABLE - HYBRID III FEMUR (BASED ON DYNAMIC TESTS SPECIFIED IN MIL-S-58095A)						
LOADING CASE	F <sub>z</sub>	F <sub>y</sub>	F <sub>x</sub>	M <sub>z</sub>	M <sub>y</sub>	M <sub>x</sub>
1	* 12592 N 2831 LB	—	—	—	—	—
2A FWD FACING	—	—	4844 N 1089 LB	394 N-m 3488 N-LB	—	720 N-m 6374 N-LB
2B SIDE FACING	10308 N 2317 LB	7218 N 1623 LB	—	—	—	2460 N-m 21776 N-LB
3	—	—	6752 N 1518 LB	—	1003 N-m 8680 N-LB	—
4	** 6516 N 1465 LB	—	7486 N 1683 LB	—	1483 N-m 13127 N-LB	—
5	** 38431 N 8640 LB	—	—	—	—	—

87 11001 15



AIR FORCE COORDINATE SYSTEM

\* TENSION

\*\* COMPRESSION

NOTES

- LOADS ARE CALCULATED FOR A FEMUR WITH A LENGTH OF 15.6 IN. FROM JOINT CENTER TO JOINT CENTER
- LOADS INCLUDE A DYNAMIC LOAD FACTOR OF 2.0 AND A SAFETY FACTOR OF 1.5
- LOADS ARE IN AIR FORCE COORDINATE SYSTEM
- THE SHADED NUMBERS REPRESENT THE CRITICAL DESIGN LOADING CASES

## 5.2 COMPONENT FEATURES

This section discusses the final design and materials used to fabricate the composite femur.

### 5.2.1 Overall Characteristics

The final design selected for the advanced composite femur is shown in Figure 4. The fabricated prototype is shown in Figure 5.

The laminated shaft was designed with an inner diameter of 1.745 in. to mate with other components. For analysis, each lamina was considered to be 0.005 in. thick, so the wall thickness for 22 plies was 0.11 in., making the outer diameter 1.965 in.

The peak axial force (Q) in a thin-walled tube subjected to pure bending can be calculated by the relationship:

$$Q = \frac{M}{\pi r^2}$$

where: Q = peak axial force (lb/circumferential in.)

M = bending moment

r = mean radius of a thin-walled tube

For the laminated shaft,

$$Q = 8,058 \text{ lb/in.}$$

$$M = 21,776 \text{ in.-lb}$$

$$r = 0.9275 \text{ in.}$$

The axial force distribution ( $F_a$ ) created by the tensile force is:

$$F_a = \frac{F_t}{2 \pi r} = 398 \text{ lb/in.}$$

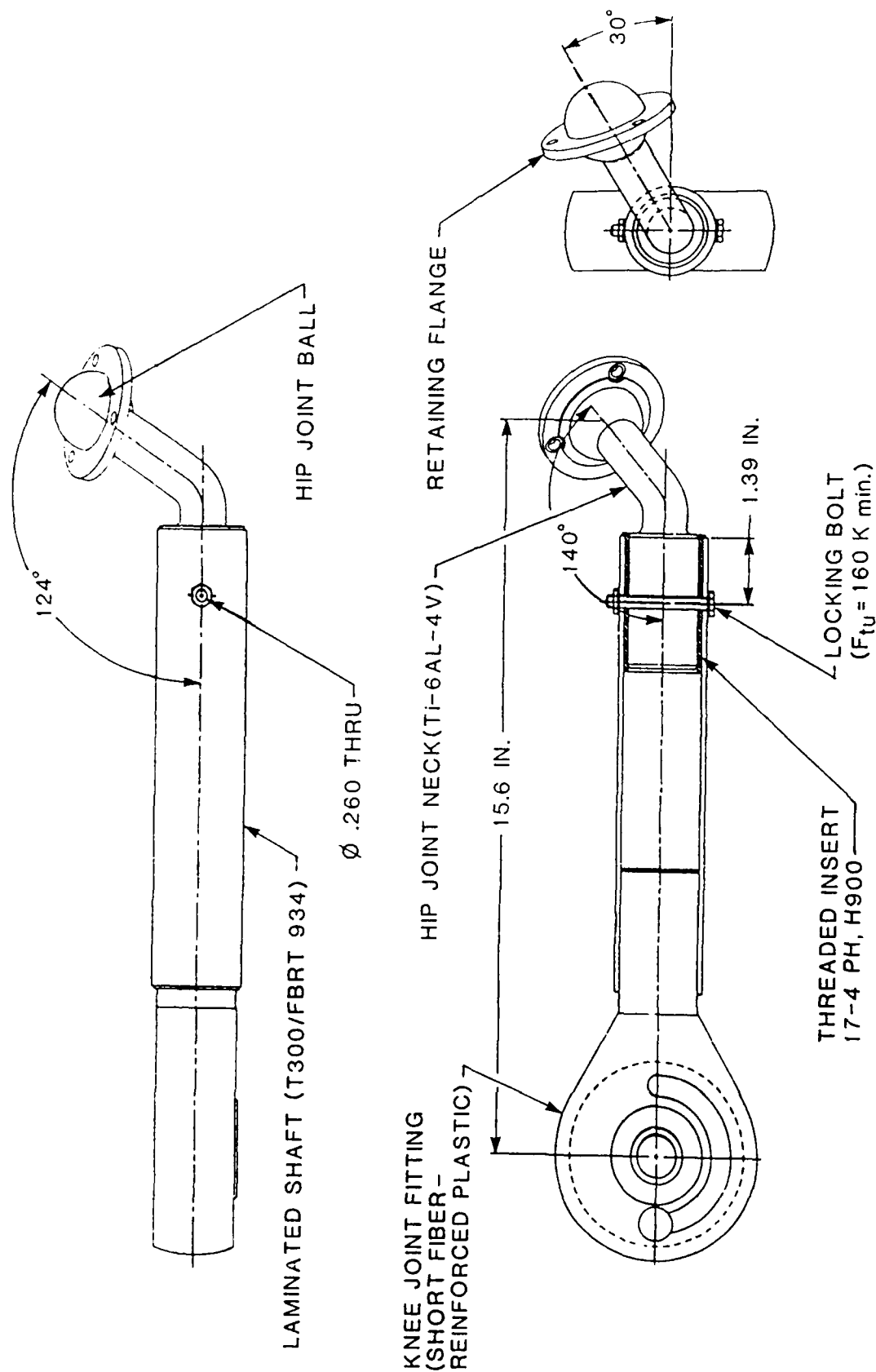


FIGURE 4. ADVANCED COMPOSITE FEMUR DESIGN.



FIGURE 5. ADVANCED COMPOSITE FEMUR PROTOTYPE.

The advanced composite femur consists of three components: the hip joint assembly, the shaft assembly, and the knee. The hip joint assembly can be disassembled from the main shaft, and the knee is permanently bonded to it. The total length of the composite femur is 18.78 in. or, from joint center to joint center, 15.65 in. The total weight of the femur is 3.9 lb, with a mass moment of inertia of 0.295 in.-lb-sec<sup>2</sup> about its transverse axes.

Both the end joints of the advanced composite femur (the hip joint ball/retaining flange and the knee) are designed similarly to those of the Hybrid III femur to provide a proper fit with the Hybrid III manikin. The axis of the composite femoral shaft, however, is offset laterally from that of the Hybrid III femur due to a change in the neck design. This change in relative position between the center of the hip joint ball and the axis of the composite shaft is more representative of the human anatomy, because the center of the ball is not directly in line with the femoral axis, whereas in the Hybrid III it is. Figure 6 illustrates this comparison.

### 5.2.2 Detailed Component Design

**5.2.2.1 Laminated Shaft Assembly.** The laminated shaft is fabricated from 22 plies of graphite/epoxy lamina (graphite T300/Fiberite 934 epoxy). The construction is midplane symmetric with the following ply orientations:

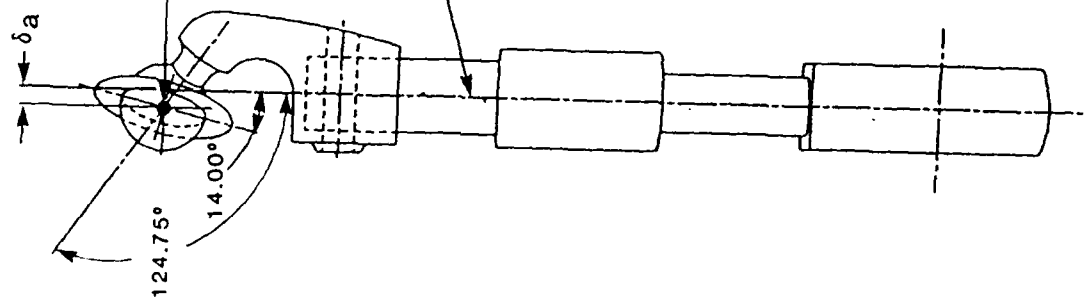
$$[0^0/30^0/0^0/-30^0/0^0/30^0/0^0/-30^0/0^0/30^0/0^0] \text{ Symmetric}$$

The critical design load, from Table 5, is loading case 2B (side-facing seat), where the loads are:

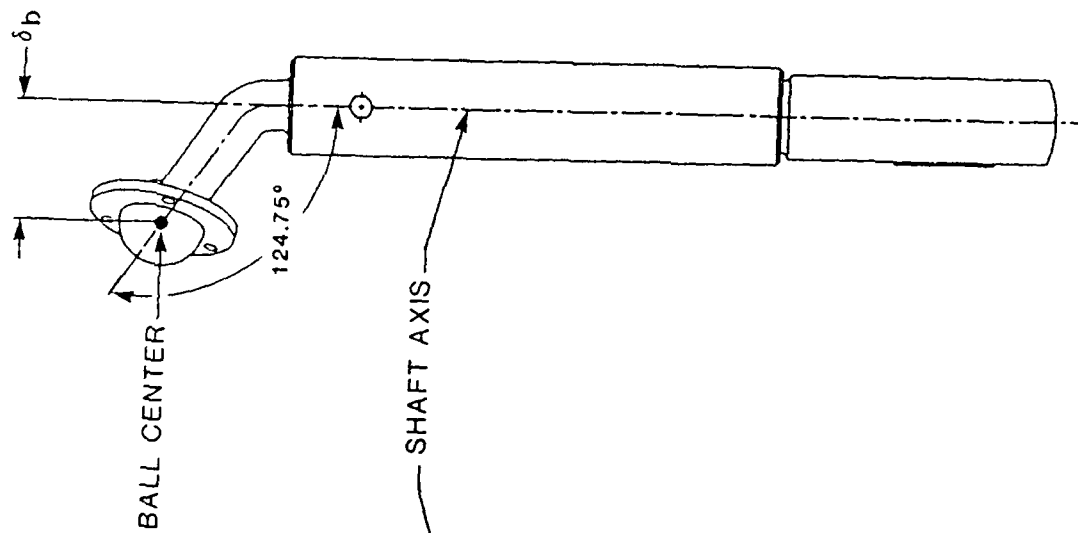
$$F_t = 2,317 \text{ lb (tension)}$$

$$F_s = 1,623 \text{ lb (shear)}$$

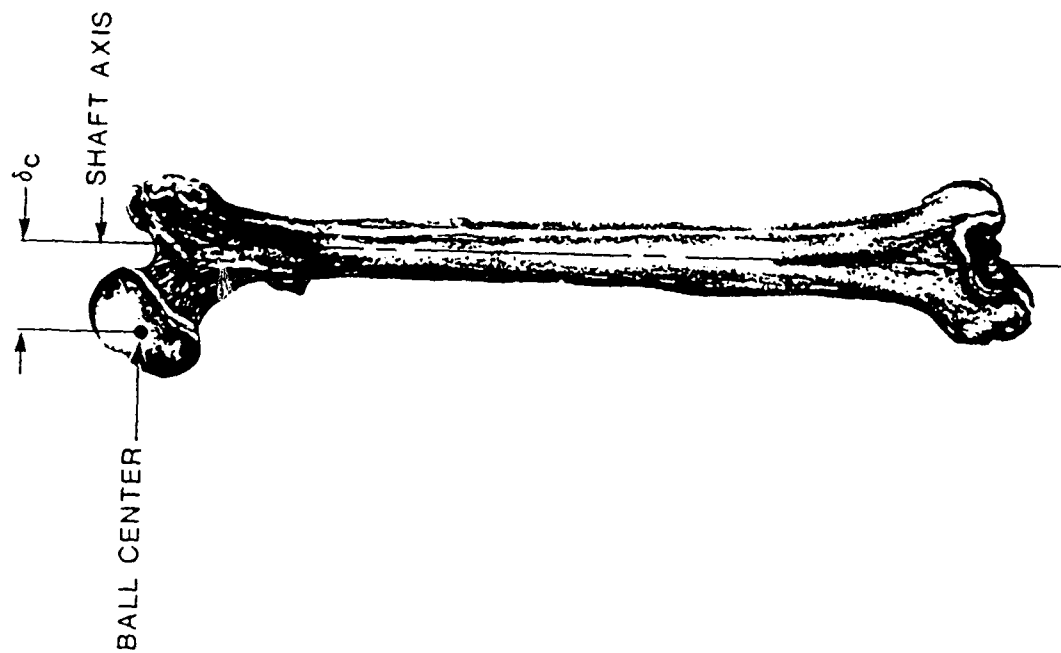
$$M = 21,776 \text{ in.-lb (bending)}$$



a. HYBRID III FEMUR



b. ADVANCED COMPOSITE FEMUR



c. HUMAN FEMUR

FIGURE 6. COMPARISON OF RELATIVE POSITION ( $\delta$ ) BETWEEN CENTER OF HIP JOINT BALL AND AXIS OF SHAFT FOR EACH FEMUR.

Therefore, the total peak axial tensile force ( $F_{a,total}$ ) due to bending plus tension is:

$$\begin{aligned} F_{a,total} &= Q + F_a \\ &= 8,456 \text{ lb/in.} \end{aligned}$$

The peak shear force ( $F_{s,total}$ ) is:

$$\begin{aligned} F_{s,total} &= \frac{F_s}{\pi r} \\ &= 557 \text{ lb/in.} \end{aligned}$$

The resulting load on a 1-in. square section of laminate is shown in Figure 7. The lamina stresses and margin of safety were calculated using the GENLAM code (Reference 7). The lamina properties used for the T300/FBRT 934 were:

$$E_x = 21.46 \times 10^6 \text{ lb/in.}^2$$

$$E_y = 1.4 \times 10^6 \text{ lb/in.}^2$$

$$E_s = 0.66 \times 10^6 \text{ lb/in.}^2$$

$$N_{uxy} = 0.30$$

$$X = 245,000 \text{ lb/in.}^2 \text{ (longitudinal tensile strength)}$$

$$X' = 226,000 \text{ lb/in.}^2 \text{ (longitudinal compressive strength)}$$

$$Y = 7,800 \text{ lb/in.}^2 \text{ (transverse tensile strength)}$$

$$Y' = 24,300 \text{ lb/in.}^2 \text{ (transverse compressive strength)}$$

$$S = 8,700 \text{ lb/in.}^2 \text{ (inplane shear strength)}$$

$$F_{xy}^* = -0.50 \text{ (} F_{xy}^* \text{ is the normalized interaction term in quadratic failure criterion)}$$

$$t = 0.005 \text{ in.}$$

The calculated strains and stresses are presented in Appendix C. The "R" ratio for each ply was calculated using the quadratic failure criterion (Reference 7). If R is greater than 1.0, failure will not occur. The calculated "R" values for each ply are also contained in Appendix C.

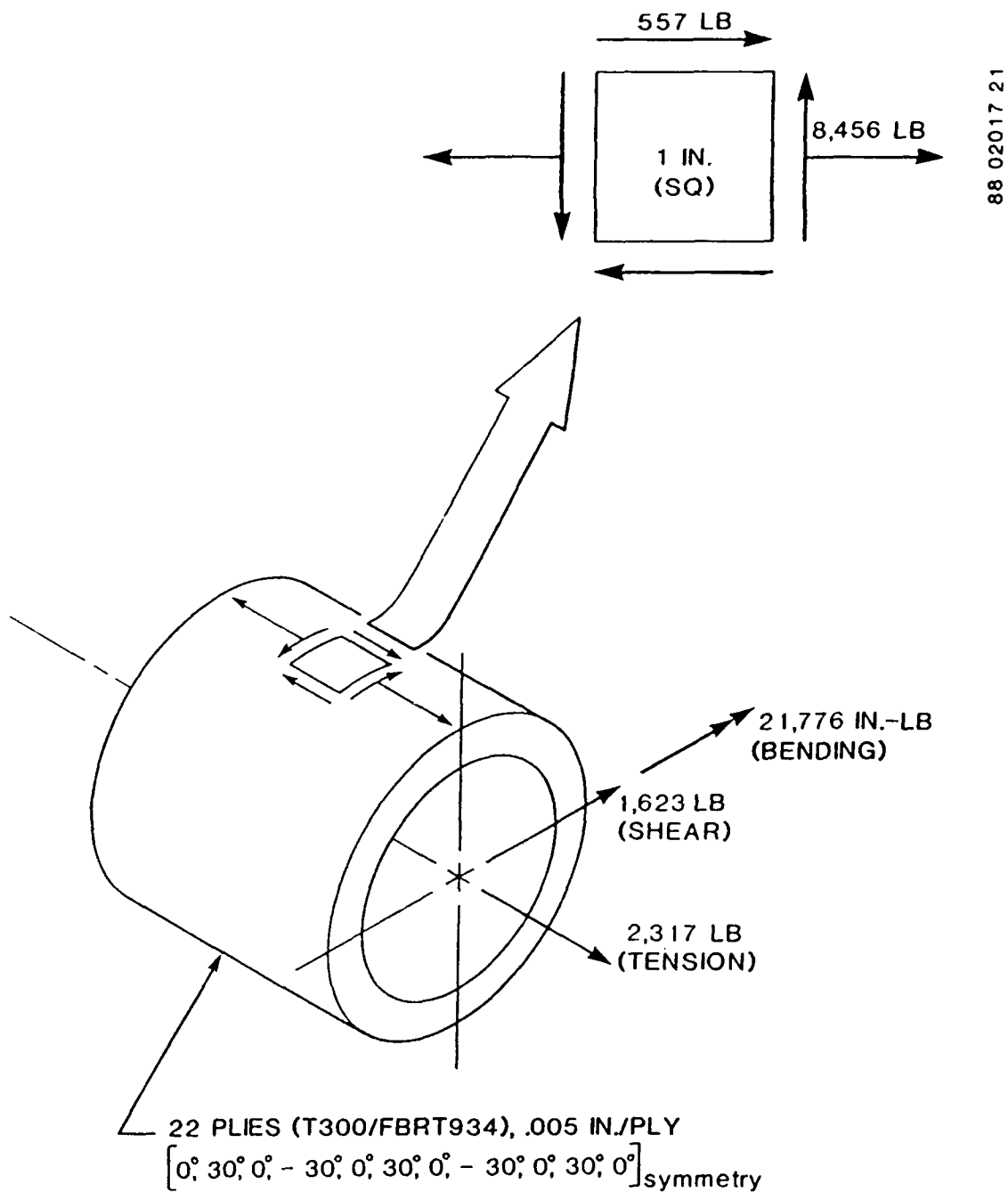


FIGURE 7. FORCES ACTING ON LAMINATED SHAFT FOR SIDE-FACING SEAT (CRITICAL LOADING CASE 2B.)

Weighing 0.51 lb, the laminated graphite/epoxy shaft prototype is 9.75 in. long with an inner diameter of 1.745 in. and an outer diameter of 2.05 in. A stainless steel (17-4 PH) threaded insert is bonded into one end of the shaft as a fitting for the neck. The adhesive used to bond the insert to the graphite shaft is Dexter Hysol 9309.3 NA epoxy. The total weight of the laminated shaft assembly is 0.79 lb. Figure 8 is an illustration of the shaft assembly.

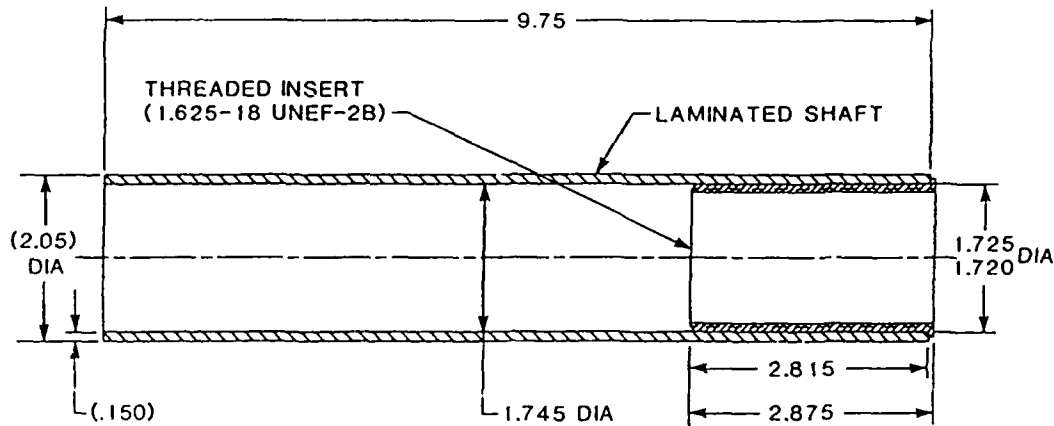


FIGURE 8. LAMINATED SHAFT ASSEMBLY.

**5.2.2.2 Knee Joint.** The knee joint fitting is machined from a block of short fiber-reinforced thermoplastic, Ultem\* 2300, which is a polyetherimide resin containing 30 percent fiberglass. Typical properties of this thermoplastic are shown in Table 6.

TABLE 6. PROPERTIES OF ULTEM 2300

Properties	Value
Tensile Strength, Yield	24,500 psi
Compressive Strength	25,500 psi
Shear Strength, Ultimate	14,000 psi
Tensile Modulus	1,300 ksi
Coefficient of Thermal Expansion (0 - 300 °F)	$1.1 \times 10^{-5}$ in./in.-°F
Specific Gravity/Density	1.51/0.0545 lb/in. <sup>3</sup>

\* Ultem is a registered trademark of General Electric Company.



The critical load for the knee joint fitting occurs during loading case 2B (see Figure 3 and Table 4). The load will be applied to the knee fitting shaft as shown in Figure 9. The resulting bending moment in the shaft is 6,718 in.-lb, which produces a stress of 13,900 lb/in.<sup>2</sup> and a margin of safety of +0.76. The detailed calculations are presented in Appendix D.

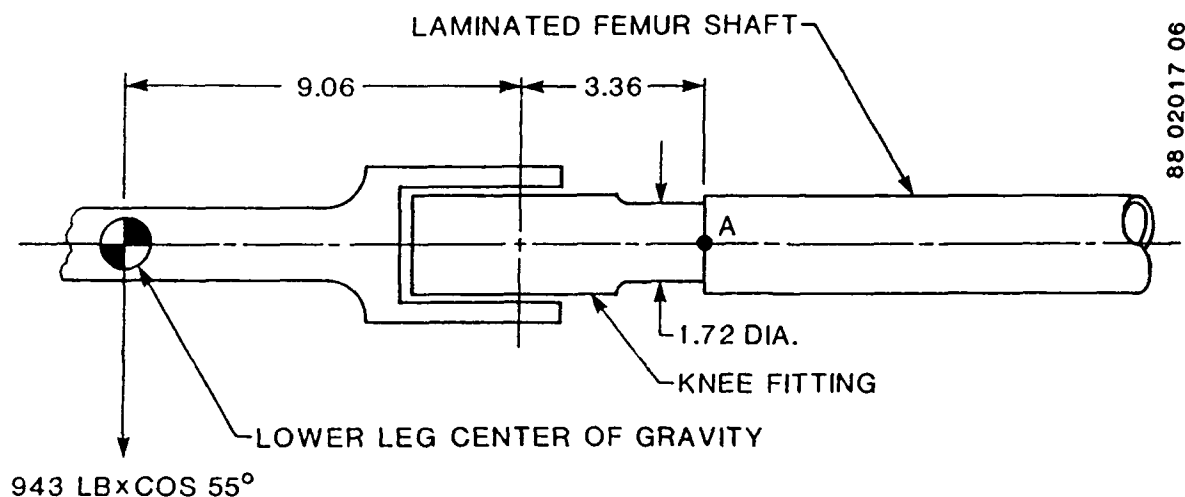
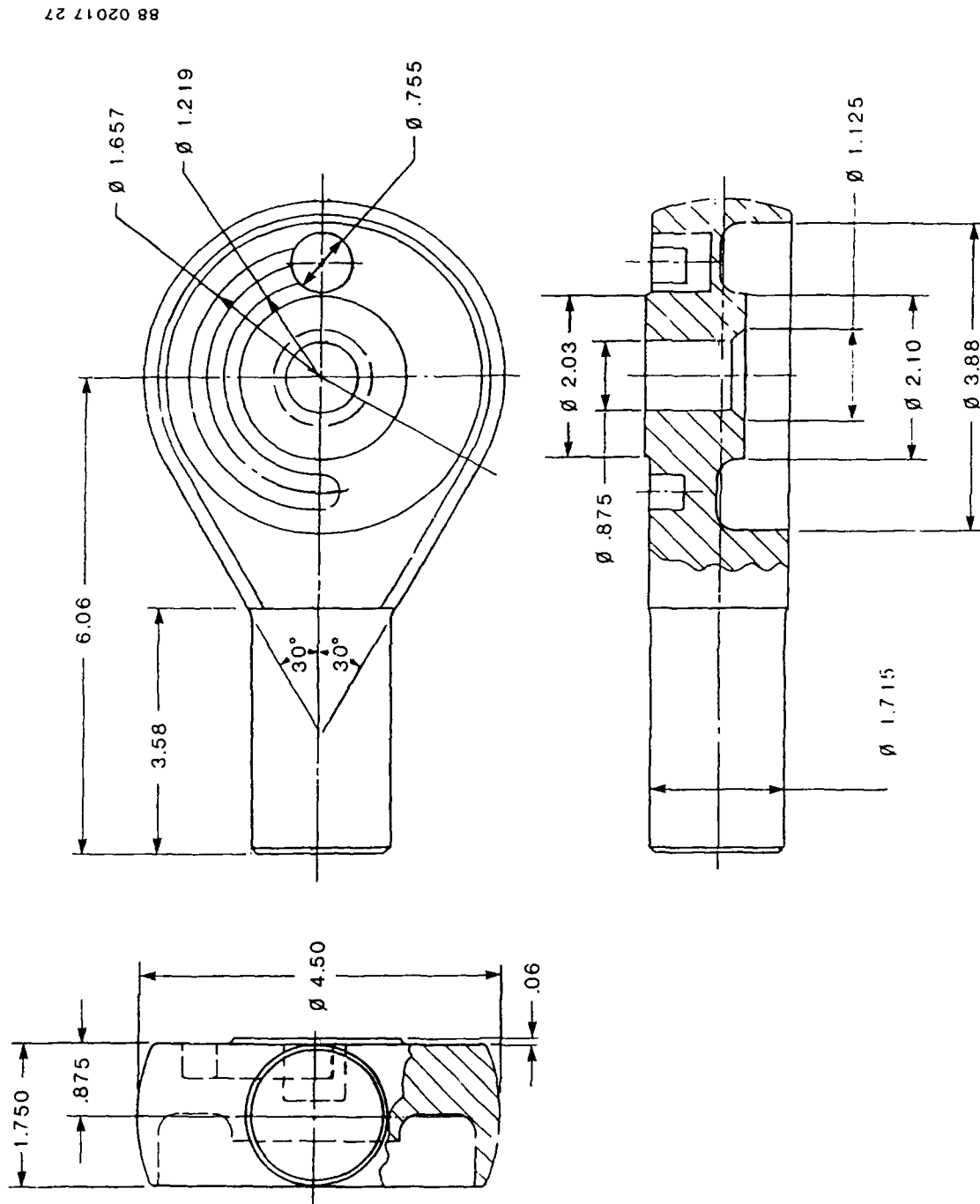


FIGURE 9. CRITICAL LOADING OF ADVANCED COMPOSITE KNEE JOINT FITTING (LATERAL LOAD - SIDE-FACING TROOP SEAT).

Conceived as an adaptation of the Hybrid III knee, the advanced composite knee was fabricated using the same dimensions, but with an extended shaft that inserts into the main shaft. Figure 10 represents the engineering drawing of the knee fitting, and Figure 11 shows the fabricated prototype. While the advanced composite knee is not optimally designed due to the design requirements to fit the Hybrid III end fittings, it is designed to withstand the critical loads. Made of a thermoplastic material, the knee fitting weighs 1.43 lb, which is 1.20 lb less than the aluminum Hybrid III knee, which weighs 2.63 lb. The composite knee is bonded directly to the inside of the graphite shaft with Dexter Hysol 9309.3 NA epoxy.

**5.2.2.3 Hip Joint Assembly.** The hip joint assembly encompasses the neck, ball joint, and retaining flange or ring (Figures 12 and 13). The neck of the existing Hybrid III manikin femur is fabricated from cast yellow brass, SAE CA863, which has an ultimate strength of 119,000 lb/in.<sup>2</sup> and a yield strength of 83,000 lb/in.<sup>2</sup> The maximum bending strength of the yellow brass neck, therefore, is 7,335 in.-lb. Calculations are included in Appendix E.



88 02017 27

FIGURE 10. ADVANCED COMPOSITE KNEE JOINT FITTING DESIGN.

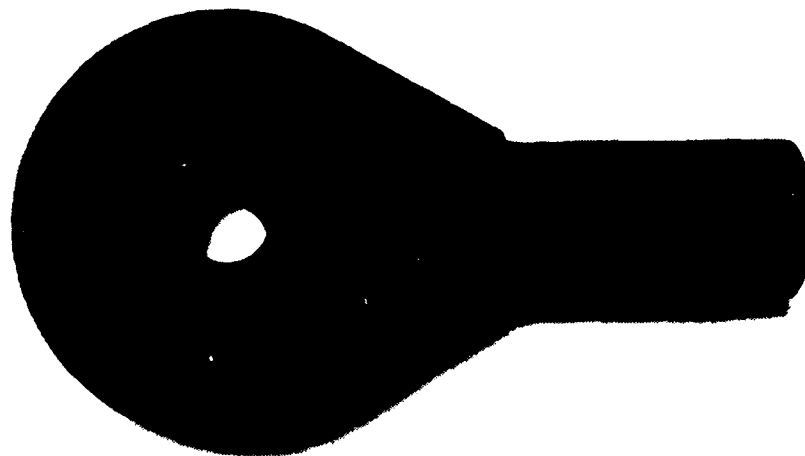


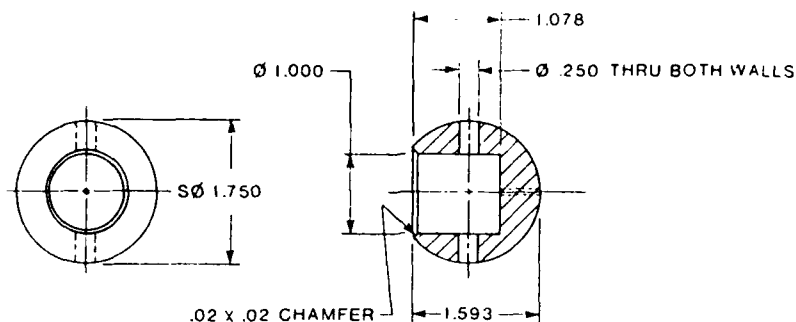
FIGURE 11. ADVANCED COMPOSITE KNEE JOINT FITTING PROTOTYPE.

Since the calculated strength of the Hybrid III neck was lower than the design strength of the laminated composite femur shaft (see Section 5.2.2.1), it was decided to strengthen the neck fitting of the composite femur as much as possible within the limitations imposed by the need to fit the existing Hybrid III hip joint socket and to hold weight to a minimum. The neck fitting was strengthened by increasing its diameter from 0.75 in. to 1.0 in. and changing its material from cast yellow brass to titanium alloy Ti-6Al-4V. Strength comparisons of these materials are shown in Table 7. In addition to the lighter weight titanium, the weight of the neck was reduced by removing unnecessary material from the center of the threaded neck base.

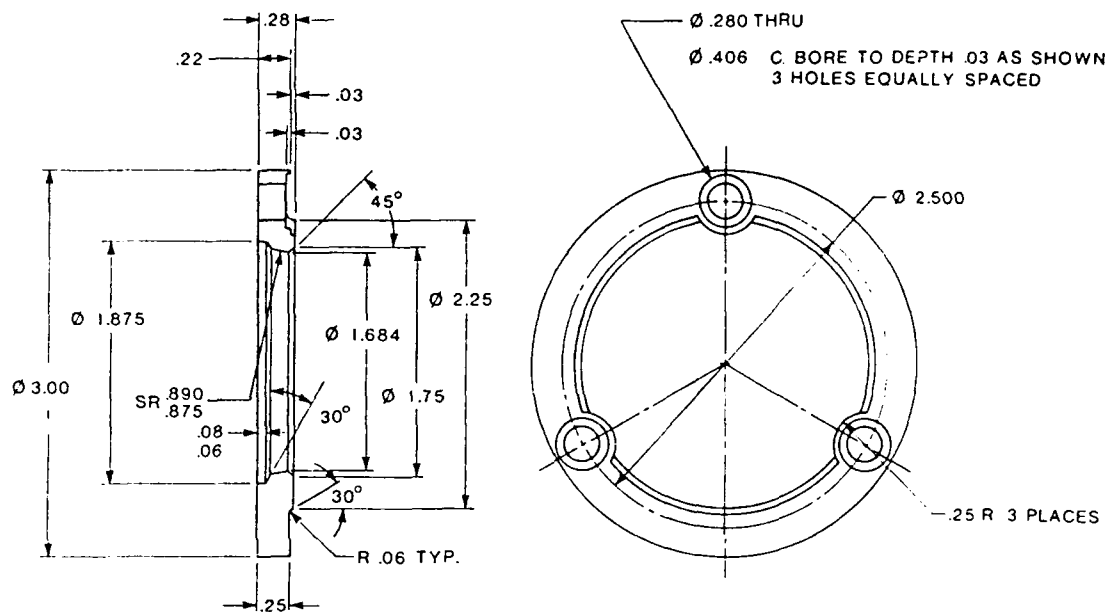
The increase in neck diameter coupled with the higher strength of titanium increased the ultimate bending strength to 22,678 in.-lb and provided an ultimate strength margin of safety of + 0.04 relative to the critical design bending moment of 21,776 in.-lb.

TABLE 7. COMPARITIVE STRENGTHS OF CAST YELLOW BRASS (SAE CA863) AND TITANIUM Ti-6Al-4V

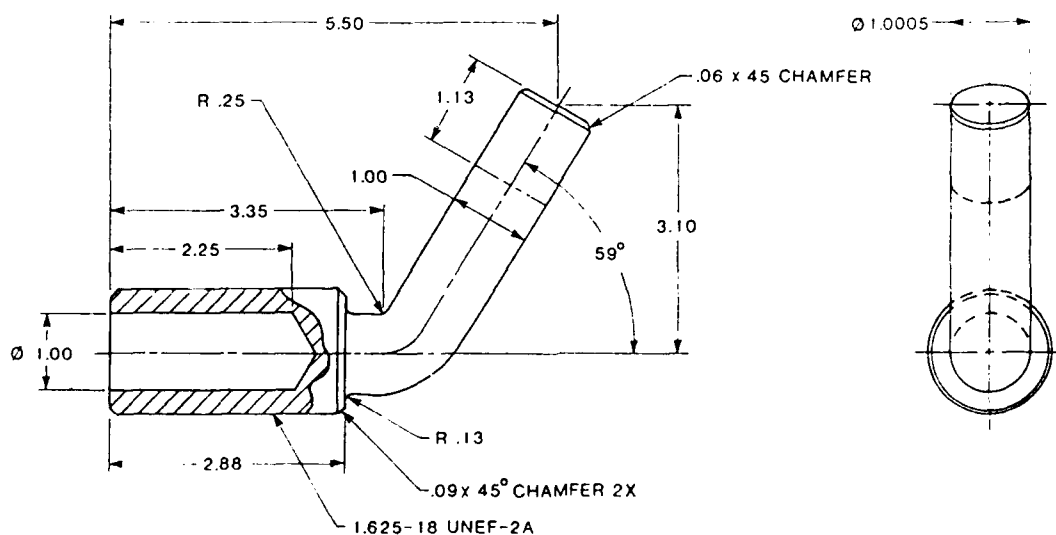
	<u>Ultimate Strength (ksi)</u>	<u>Yield Strength (ksi)</u>
Cast Yellow Brass	119.0	83.0
Ti-6Al-4V	140.0	130.0



a. HIP JOINT BALL



b. RETAINING FLANGE

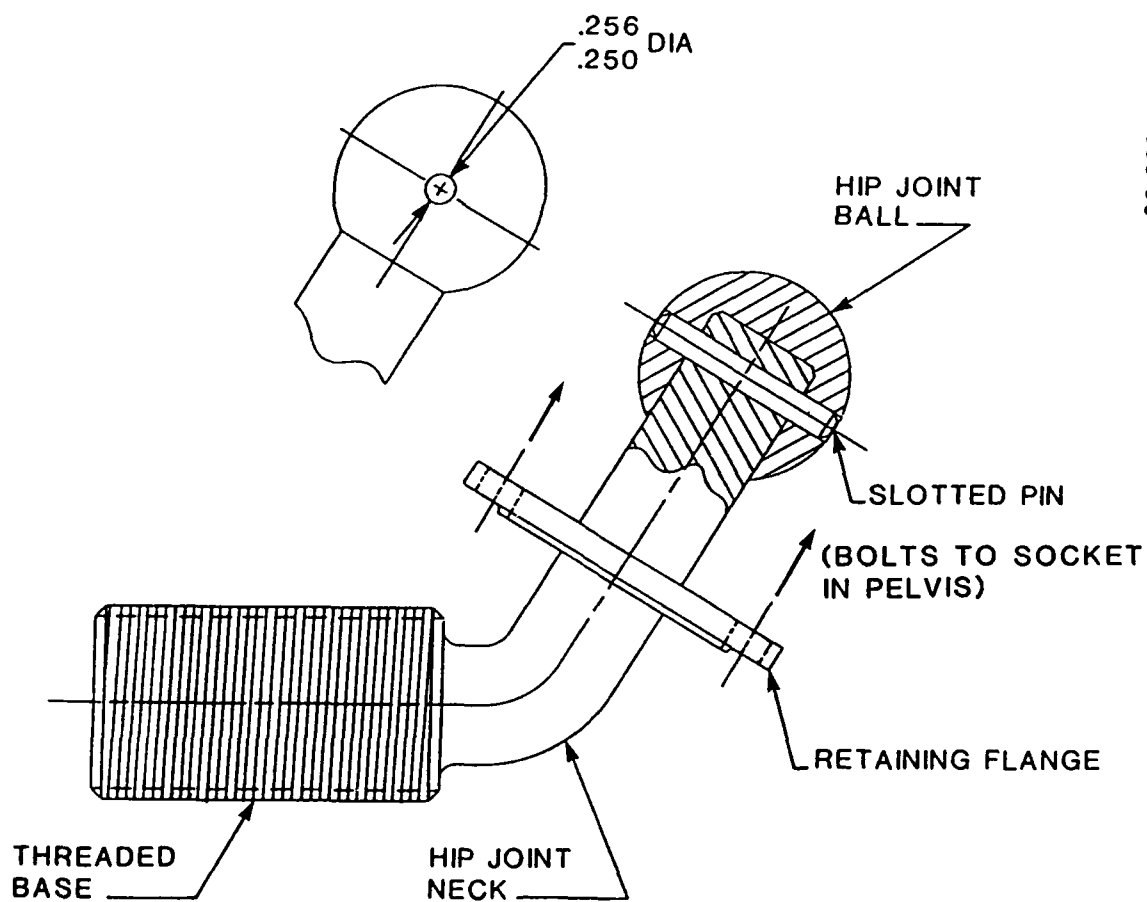


c. HIP JOINT NECK FITTING

FIGURE 12. SUBCOMPONENTS OF THE HIP JOINT ASSEMBLY.



88042-20



88 02017 08

FIGURE 13. ADVANCED COMPOSITE HIP JOINT ASSEMBLY.

The configuration of the composite femur neck does not incorporate the curve of the Hybrid III neck, thus increasing the distance between the center of the hip ball joint and the axis of the shaft. This configuration, as discussed in Section 5.2.1, is a better anatomical representation of the human femur (Figure 6). However, due to the increased neck diameter, the allowable degree of rotation of the hip joint was reduced from that of the Hybrid III. Therefore, the thickness of the retaining flange was reduced to accommodate the increase in neck diameter and maintain original hip joint rotation. In the Hybrid III, the ring flange is made of aluminum bronze, which has a tensile strength of 110 ksi. To reduce the chance of failure, the retaining flange for the advanced composite femur was made from 17-4 PH stainless steel, which has a strength of 200 ksi.

The hip joint ball was changed from that of the Hybrid III only by increasing the diameter of the hole into which the neck is inserted from 0.75 in. to 1.0 in. The ball is made from aluminum bronze and has a diameter of 1.75 in.

### 5.2.3 Weight and Center of Gravity

The weight and center of gravity for the composite femur were calculated. Table 8 lists the weight of each component of the advanced composite femur. Tables 9 and 10 list the mass and mass moments of inertia of the femur and upper leg for the human, Hybrid III, and composite prototype.

The design goal was to match the weight and moments of inertia of the composite femur and the 50th-percentile human upper leg. To meet this goal, the artificial skin used with the composite femur must have a mass of 17.84 lb and mass moments of inertia about the transverse axes of 1.15 in.-lb-sec<sup>2</sup>. Figure 14 depicts the location of the center of gravity for the femur and flesh and presents the mass and mass moments of inertia of the combined part.

### 5.2.4 Recommended Flesh Design

Although not a contractual requirement, Simula undertook a preliminary study to recommend a flesh design that would be compatible with the advanced composite femur. Since the weight of the composite femur is reduced from that of the Hybrid III femur by 70 percent, the weight of the flesh must be increased to achieve the appropriate total weight of the upper leg. This shift in weight from the skeletal component to the flesh covering will provide an upper leg with a more representative weight distribution and resulting inertial properties.

As shown in the weight analysis (Section 5.2.3), the composite femur weighs 3.94 lb, but the total upper leg must weigh 21.56 lb to achieve the proper human leg weight. Therefore, the flesh must be designed to weigh 17.62 lb. Similarly, the mass moments of inertia about the transverse axes of the composite femur is 0.295 in.-lb-sec<sup>2</sup> and that of the total upper leg of the human is 1.46 in.-lb-sec<sup>2</sup>. The mass moments of inertia of the thigh must therefore be 1.15 in.-lb-sec<sup>2</sup> (see Figure 14). Measured from the center of the hip joint ball, the center of gravity of the flesh covering is 7.88 in. In addition, the outside dimension of the flesh covering, from the back of the thigh to the front, should not exceed 6.58 in. (Reference 8). Assuming that the flesh surrounds the composite femur concentrically, the necessary

TABLE 8. WEIGHTS OF ADVANCED COMPOSITE  
FEMUR COMPONENTS

Component	Weight	
	(kg)	(lb)
Aluminum Bronze Ball	0.228	0.502
Pin	0.007	0.015
Titanium Neck	0.516	1.135
Threaded Insert (17.4 PH)	0.125	0.275
Graphite/Epoxy Shaft	0.232	0.510
Adhesive In Shaft (9309.3 NA)	0.004	0.009
Bolts (2)	0.011	0.025
Nuts (2)	0.002	0.004
Washers (8)	0.007	0.015
Ultem 2300 Knee	0.657	1.433
Adhesive on Knee	0.006	0.013
Stainless Steel Retaining Flange	<u>0.143</u>	<u>0.315</u>
TOTAL*	1.789	3.936

\*Total value does not include the weight of the stainless steel retaining flange (0.315 lb) since it does not contribute to the inertial properties of the femur.

TABLE 9. UPPER LEG AND FEMORAL MASS FOR  
HUMAN, HYBRID III AND COMPOSITE  
PROTOTYPE (LB)

	<u>Femur</u>	<u>Upper leg (Femur and Flesh)</u>
Human	1.9(1)	21.56(2)
Hybrid III	12.5(3)	19.99(4)
Composite	3.9(3)	21.56(5)

1. Experimental analysis of human femur
2. Reference 8
3. Actual measure
4. Reference 9
5. Design goal

TABLE 10. UPPER LEG AND FEMORAL MASS MOMENTS OF INERTIA  
(IN.-LB-SEC<sup>2</sup>)

	<u>Femur</u>	<u>Upper Leg (Femur and Flesh)</u>		
		<u>I<sub>x</sub></u>	<u>I<sub>y</sub></u>	<u>I<sub>z</sub></u>
Human	0.209(1)	1.46(2)	1.46(2)	0.40(2)
Hybrid III	0.962(4)	1.45(3)	1.50(3)	0.20(3)
Composite	0.295 (4)	1.46(5)	1.46(5)	0.40(5)

1. Experimental analysis of human femur
2. Reference 8
3. Reference 9
4. Theoretical analysis
5. Design goal

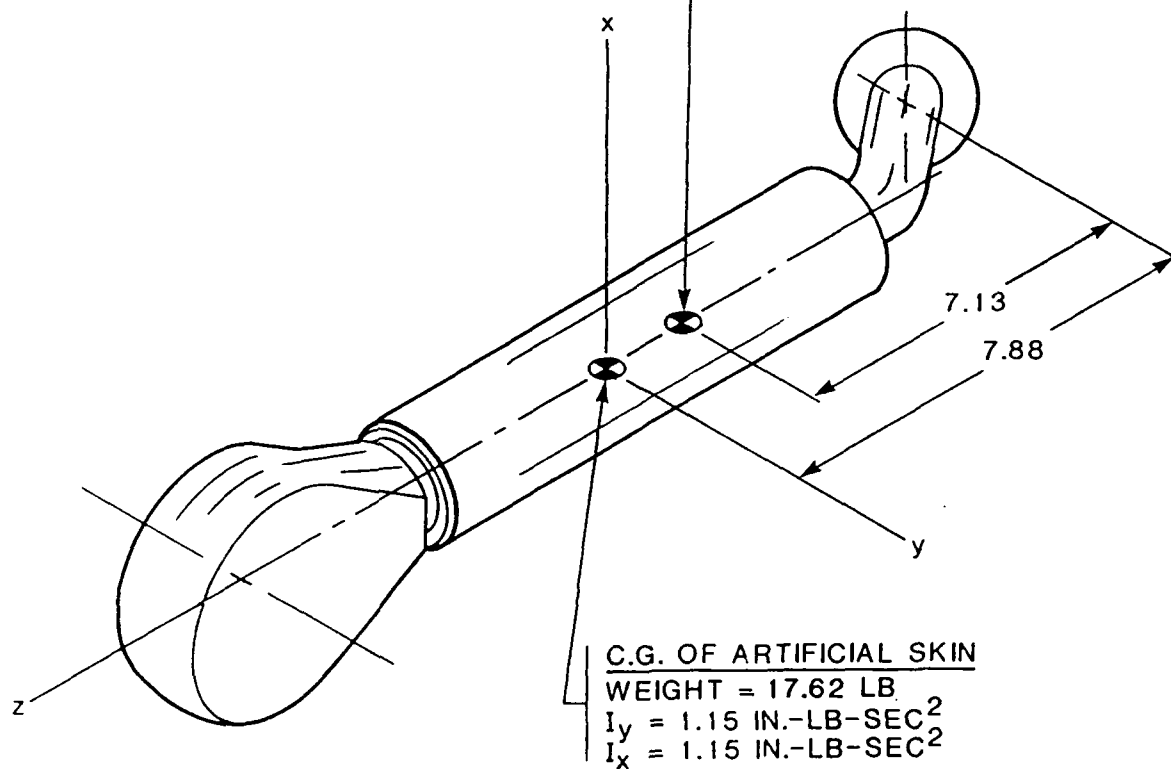


C.G OF ADVANCED COMPOSITE  
FEMUR ASSEMBLY

WEIGHT = 3.94 LB

$I_y = I_x = .295 \text{ IN.-LB-SEC}^2$

88 02017 09



C.G. OF ARTIFICIAL SKIN

WEIGHT = 17.62 LB

$I_y = 1.15 \text{ IN.-LB-SEC}^2$

$I_x = 1.15 \text{ IN.-LB-SEC}^2$

COMBINED PROPERTIES OF  
SKIN AND FEMUR

WEIGHT = 21.56 LB

$I_y = 1.46 \text{ IN.-LB-SEC}^2$

$I_x = 1.46 \text{ IN.-LB-SEC}^2$

FIGURE 14. REQUIRED LOCATION, WEIGHT, AND MOMENTS OF INERTIA  
OF ADVANCED COMPOSITE FEMUR.

density of the flesh covering was calculated to be 0.0338 lb/in.<sup>3</sup> or 0.936 specific gravity. Table 11 lists those materials with densities similar to the desired density of 0.936 specific gravity. In addition to material density, the compliance and energy absorption of the material should be considered to properly represent human flesh.

TABLE 11. POTENTIAL FLESH COVER MATERIALS

<u>Material</u>	<u>Specific Density</u>
Desired Density (Composite Flesh)	0.936
Natural Polypropylene	0.91
UHMWPE, Virgin	0.94
Natural/Synthetic Rubber	0.93
Butyl Rubber	0.95
Polysulfide	1.40
- Filled with Microspheres	0.94
Ultrawear UHMWPE	0.94
Polypropylene	0.90

Figure 15 shows the flesh design that would be most suited to the composite femur. The concept consists of three composite, circular discs that are hinged on one side so as to be able to encircle the femoral shaft. Flanges provide the surface needed to bond each disc to the shaft. Figure 16 illustrates this concept. The flesh would need to be molded from a recommended material with cavities that encase the discs. The purpose of these discs is to prevent the mass of the flesh from slipping along the skeletal component under high inertial loads.

The recommended flesh covering is conceptualized with features similar to that of the ADAM even though it weighs approximately twice as much as the ADAM flesh. The recommended flesh cover is folded around the femur and sealed. The means of sealing the flesh will be determined by the strength requirements. If a zipper is adequate, as it appears to be for the ADAM, then one will be used. Figure 17 demonstrates how the outer skin of the flesh covering of the lower leg of the ADAM is formed first and then

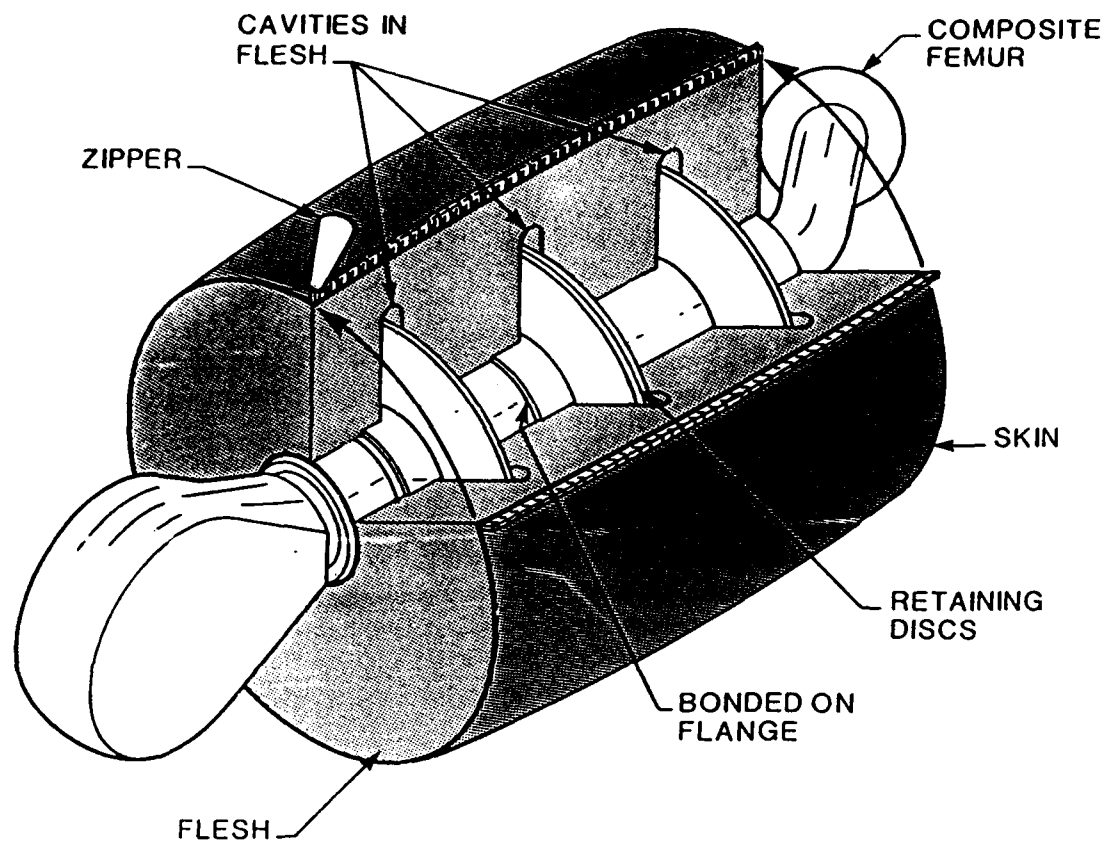


FIGURE 15. DESIGN OF RECOMMENDED FLESH COVERING.

injection molded with a foam to represent the flesh. It is probable that the flesh will have to be ballasted to produce the proper overall weight and mass moment of inertia. This recommended concept can also be applied to future developmental composite skeletal components.

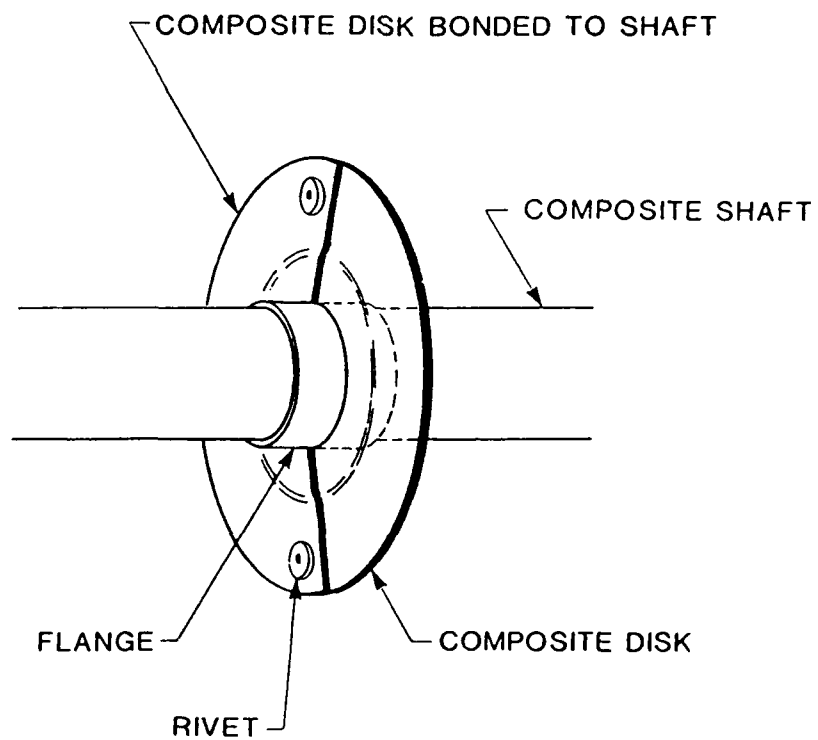
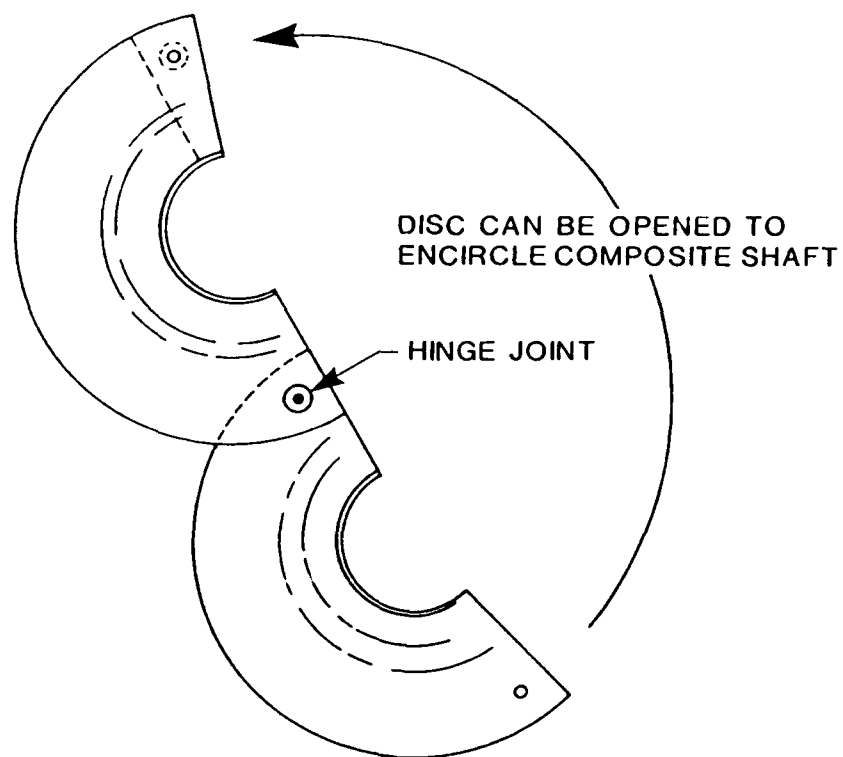


FIGURE 16. COMPOSITE DISC FOR RETENTION OF FLESH COVERING.

88024-8

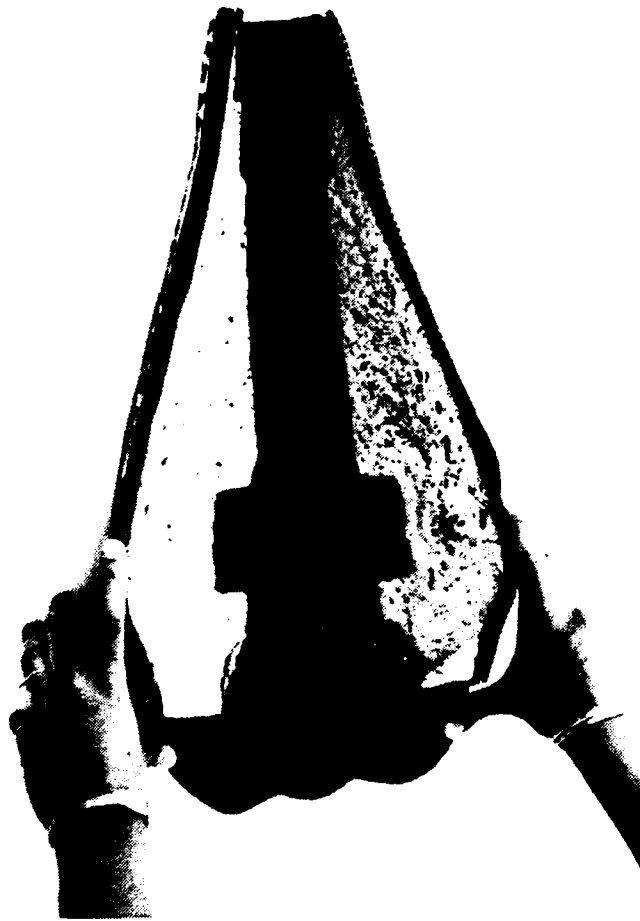


FIGURE 17. FLESH COVERING OF LOWER LEG OF ADAM.

## 6.0 MECHANICAL TESTING

### 6.1 PURPOSE

The advanced composite femur was statically tested to determine whether it would sustain the maximum applied loads expected in service. The most severe femoral loads, as calculated in Appendix B and tabulated in Table 5, were selected for testing.

The static loads included a dynamic factor of 2.0 and a safety factor of 1.5, and were applied to test the torsional strength, the compressive strength, the bending strength, and the combined bending and tensile strength of the composite knee and shaft. The titanium neck was subjected to a lateral bend test. Although the neck was designed to sustain higher loads than could be sustained by the original Hybrid III neck fitting, its strength could not be designed to equal or exceed that produced by the graphite shaft. This strength limitation was due to the space limitations within the existing Hybrid III pelvis structure. Therefore, the titanium neck was tested independently from the knee and shaft.

### 6.2 TEST PLAN

The test plan consisted of four static tests of the composite knee and shaft and one test of the titanium neck. Each test was designed to use the same composite femur in order to provide an analysis of its overall strength.

Test 1 was designed to test the torsional strength of the knee and laminated shaft. A 565-lb load was applied to a moment arm on the knee to produce a torque of 3,488 in.-lb to the shaft (Figure 18). This test represented the critical torque in load case 2A (Table 5).

Test 2 was designed to test the axial compressive strength of the knee and shaft assembly (Figure 19). A ramped input compressive load was applied axially at the end of the knee up to the critical load of 8,640 lb, as found in load case 5 (Table 5).

Test 3 was a bending test of the composite shaft, designed to reach the critical load of 21,776 in.-lb in load case 2B (Table 5). A force of 1,230 lb was applied to a moment arm at the knee to create the critical load at point b (Figure 20). Point b represents the hip-joint ball center which is designed to withstand the critical load. The laminated shaft was tested to a critical moment of 18,708 in.-lb at point c.

Test 4 (Figure 21) combines the lateral and tensile forces found in load case 2B (Table 5). A force of 2,623 lb was applied at an angle of  $28^{\circ}$  to the longitudinal femoral axis to produce the critical moment of 21,776 in.-lb and a tensile load of 2,317 lb.

Test 5 tested the strength of the titanium neck. The titanium neck was tested anatomically to represent the lateral load case 2B (Table 5) by attaching it to a test fixture at the ball joint on one end and to the composite shaft on the other end. A load of 1,512 lb was applied to the end of the shaft at a distance that represented center of the knee, to produce the critical moment of 21,776 in.-lb in the center of the hip joint ball (Figure 22).

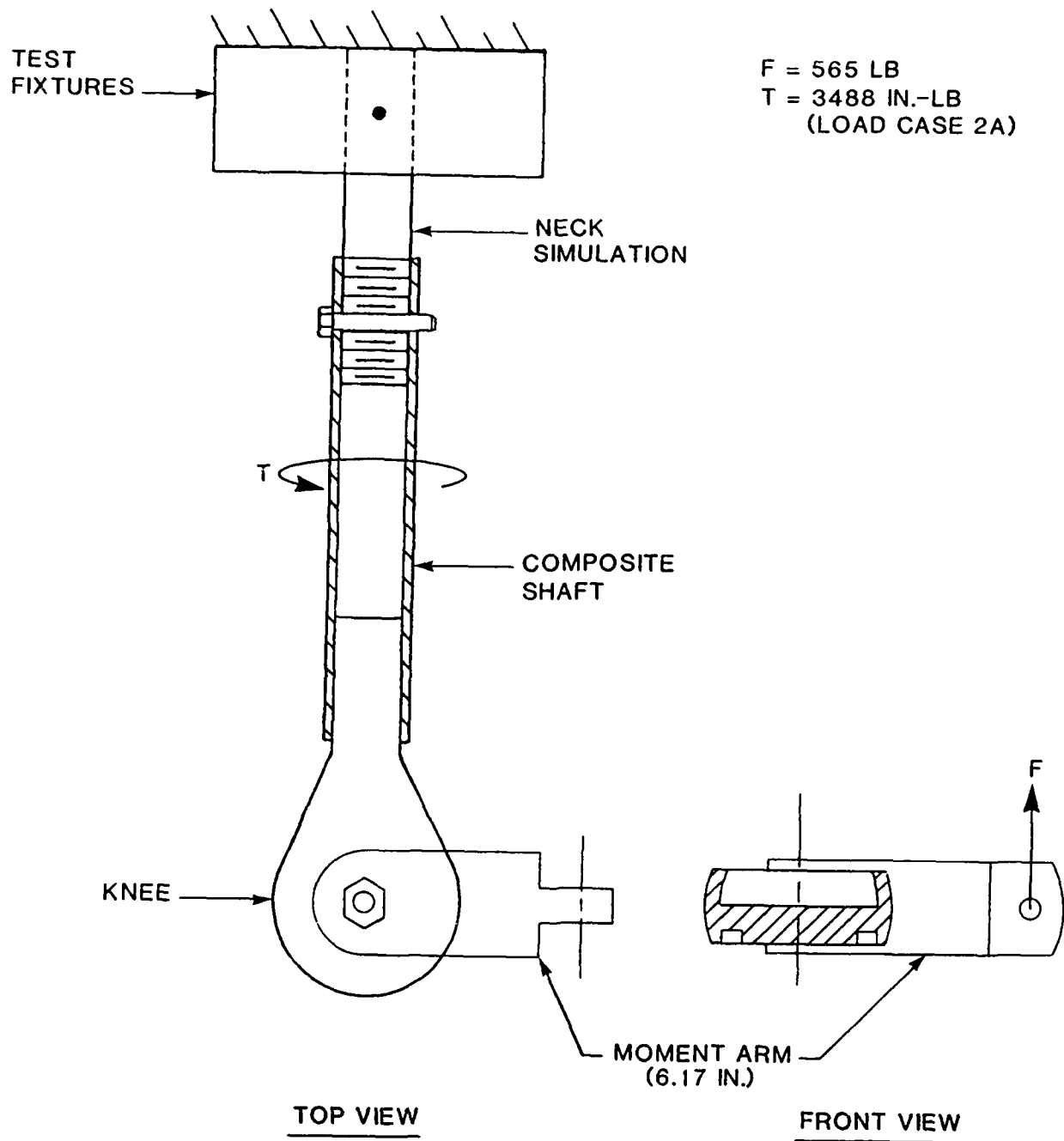
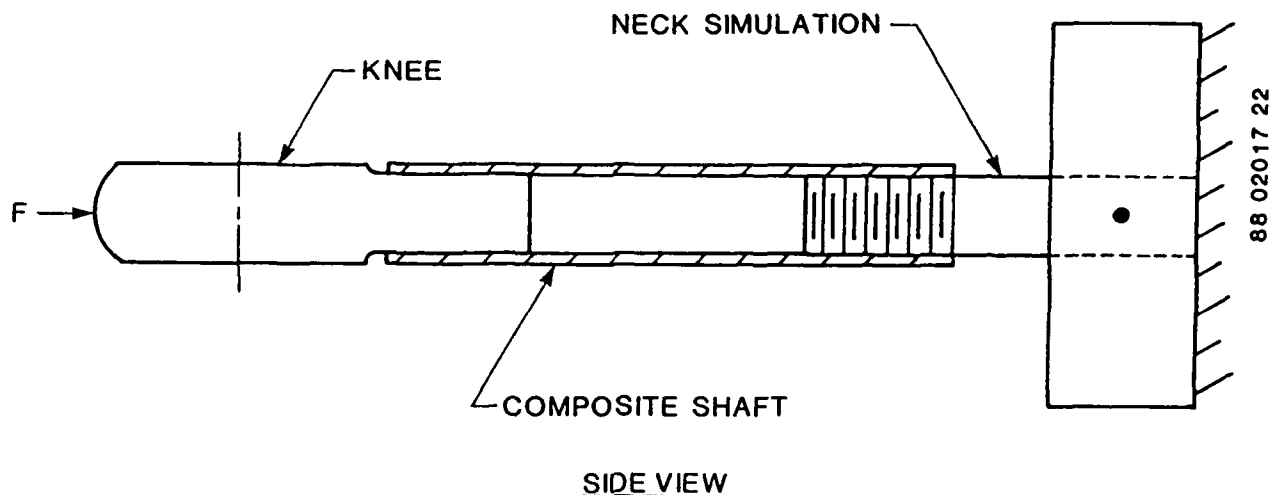


FIGURE 18. TEST 1 - TORSION.



F = 8,640 LB (LOAD CASE 5)

FIGURE 19. TEST 2 - COMPRESSION.

### 6.3 TEST RESULTS

The final test results are tabulated in Table 12. These results do not reflect the design support tests which are included in the discussion.

#### 6.3.1 Test 1 - Torsion

The composite graphite shaft and the thermoplastic knee were tested up to a 3,517 in.-lb torque along the axis of the femur. The critical torque of 3,488 in.-lb was exceeded by nearly one percent without failure. Figure 23 shows the component following the test.

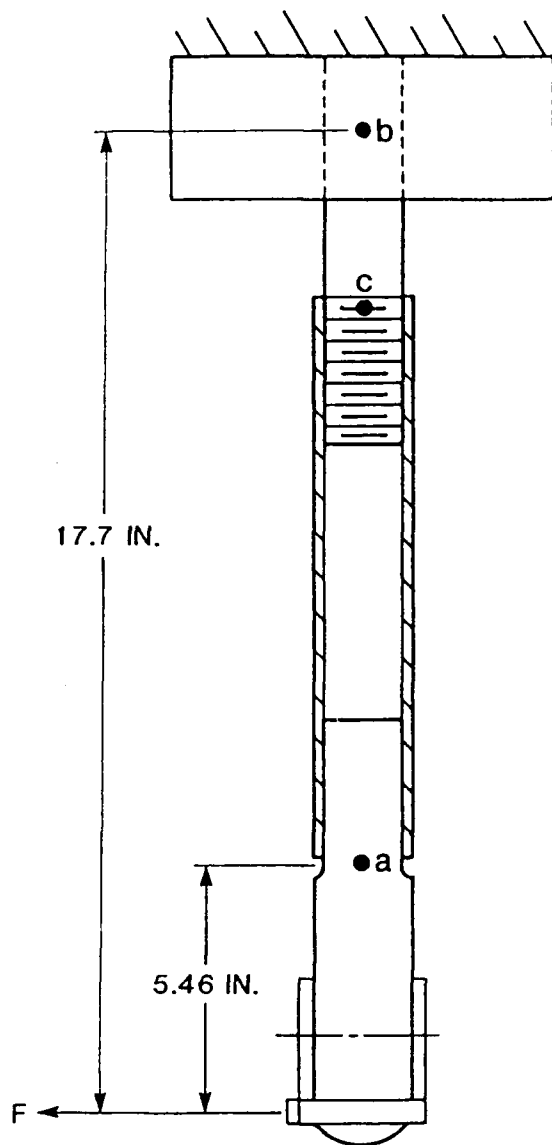
#### 6.3.2 Test 2 - Compression

The same two femoral components tested in Test 1 were subjected to a 9,114.6 lb compression load, which exceeded the design load of 8,640 lb by 5 percent. Both components successfully passed the test.

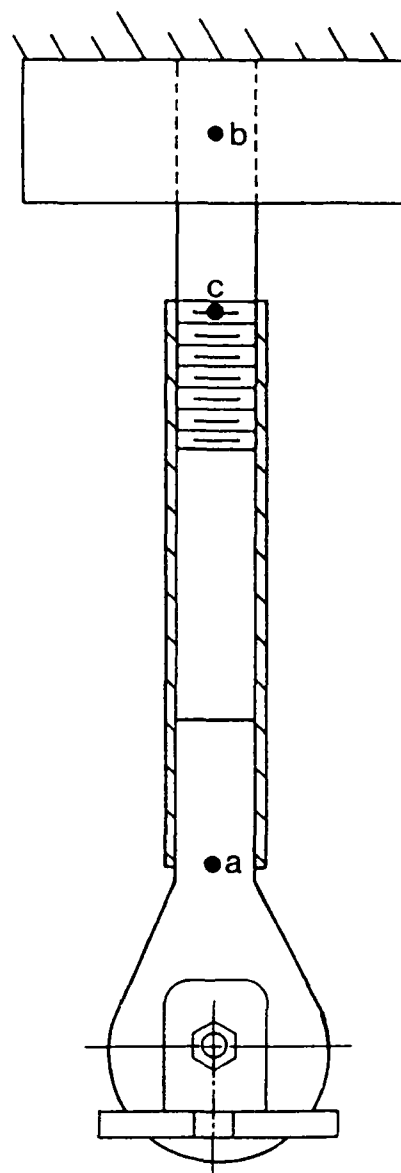
#### 6.3.3 Test 3 - Combined Lateral Bending/Torsion

This test, which was designed to represent the loads in a side-facing troop-seat, caused the knee to fail at the knee shaft at only 40 percent of its designed strength. The direct cause of this failure was attributed to a poor bond between the knee and graphite shafts resulting in ultimate failure. The bond surfaces between the two shafts were improved for subsequent test items. This test was not repeated as it was believed that Tests 4 and 5 would adequately evaluate the structural integrity of the knee shaft.

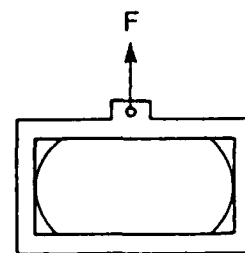




SIDE VIEW



TOP VIEW

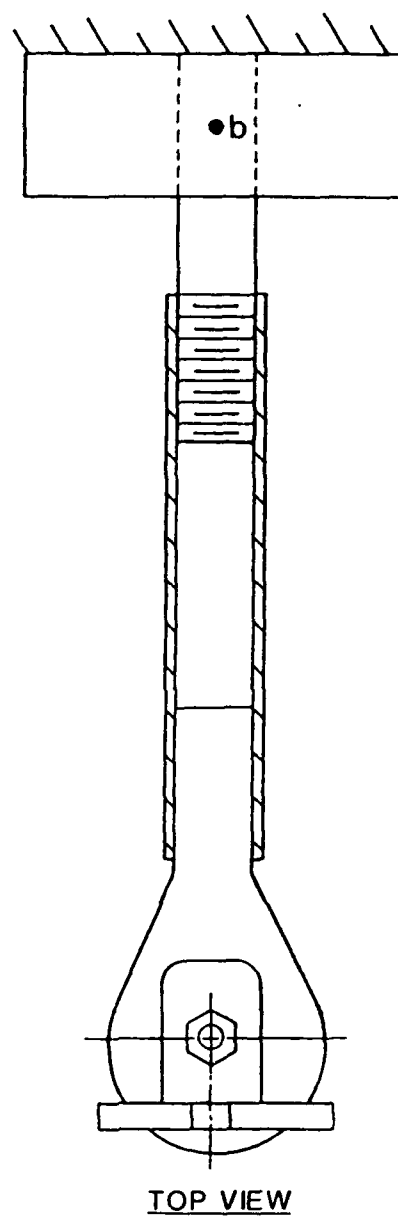
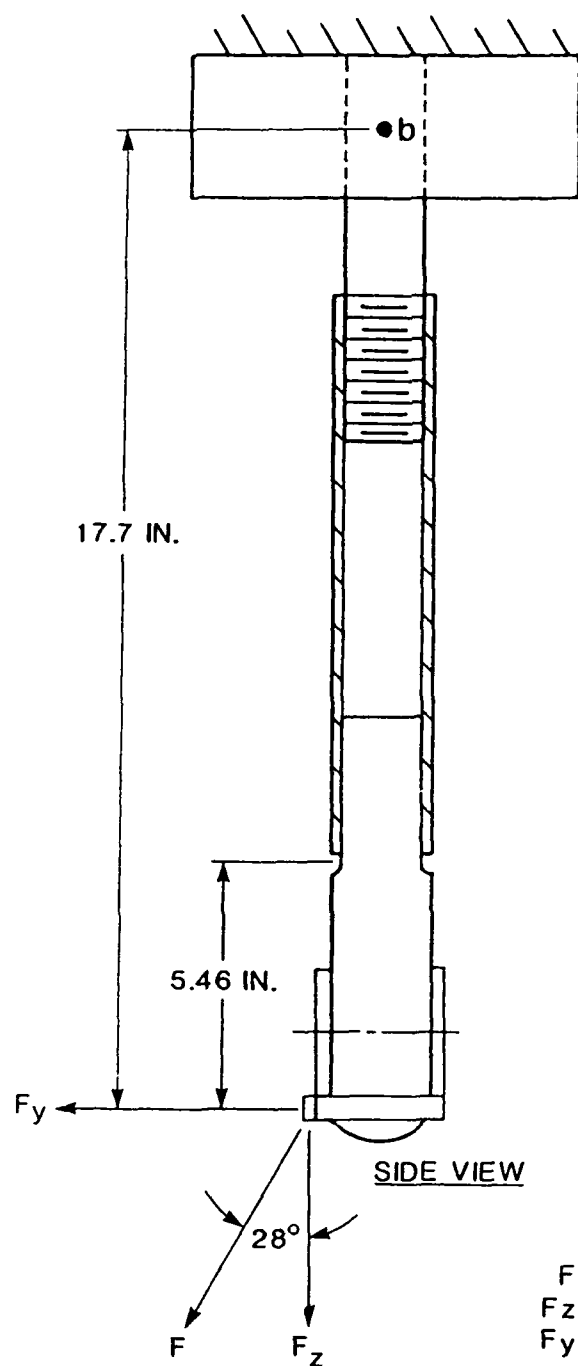


FRONT VIEW

$F = 1,230 \text{ LB}$   
 $M_a = 6,718 \text{ IN.-LB}$   
 $M_b = 21,776 \text{ IN.-LB (LOAD CASE 2B)}$   
 $M_c = 18,708 \text{ IN.-LB}$

88 02017 25

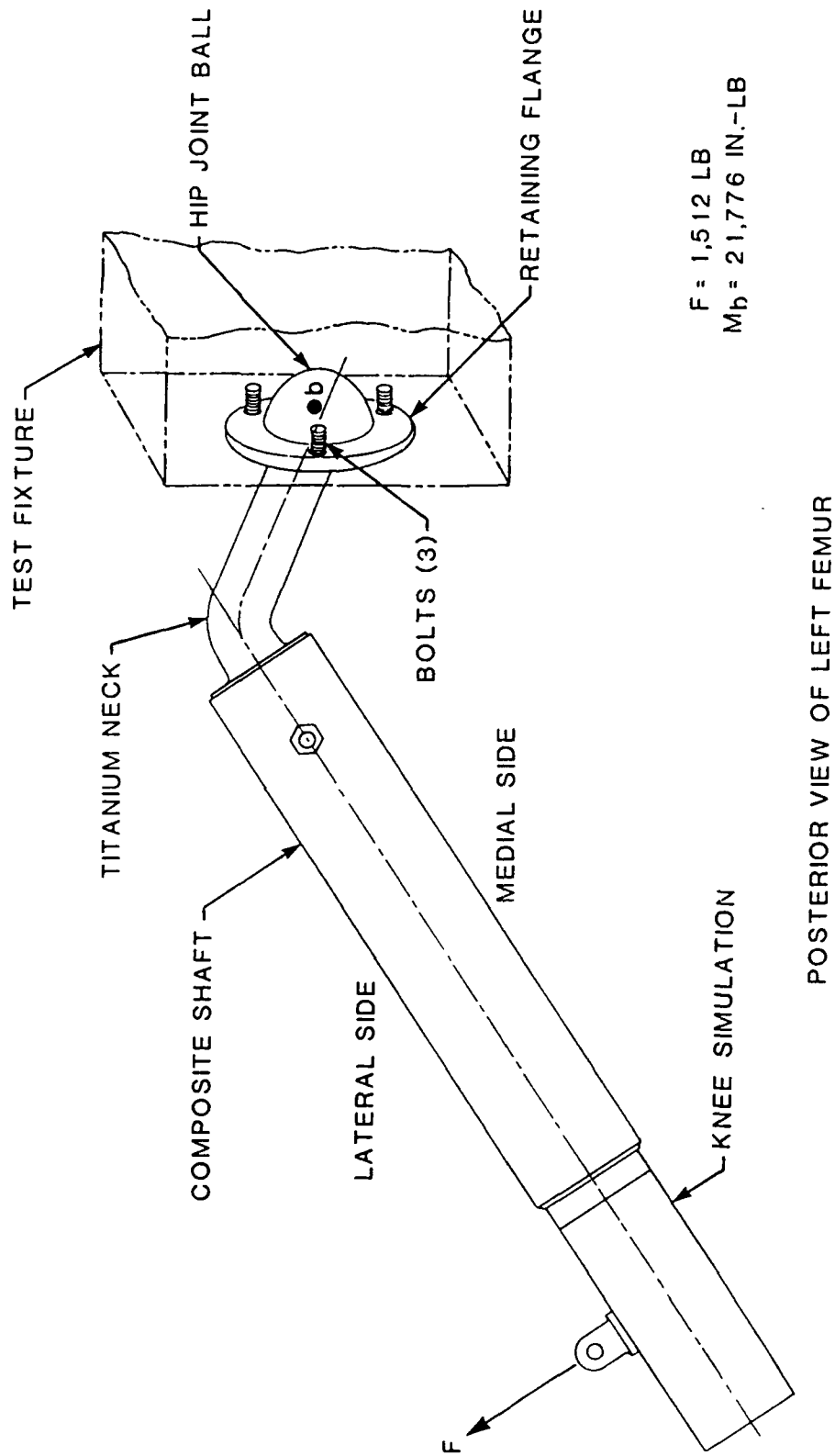
FIGURE 20. TEST 3 - BENDING.



88 02017 23

$F = 2,623 \text{ LB}$   
 $F_z = 2,317 \text{ LB (LOAD CASE 2B)}$   
 $F_y = 1,230 \text{ LB (LOAD CASE 2B } M_x = 21,776 \text{ IN.-LB)}$

FIGURE 21. TEST 4 - COMBINED BENDING/TENSION.



$F = 1,512 \text{ LB}$   
 $M_b = 21,776 \text{ IN.-LB}$

POSTERIOR VIEW OF LEFT FEMUR

FIGURE 22. TEST 5 - LATERAL BEND TEST OF TITANIUM NECK.

TABLE 12. FINAL STATIC TEST RESULTS ON COMPOSITE FEMUR\*

Test	Design Load	Actual Load	Result
1. Torsion	565 lb 3,488 in.-lb	570 lb 3,517 in.-lb	Test Pass
2. Axial Compression	8,640 lb	9,115 lb	Test Pass
3. Knee Bend	6,718 in.-lb	6,750 in.-lb	Test Pass
4. Neck Bend	21,776 in.-lb	18,043 in.-lb	- Existing Hybrid III bolt failed - By analysis proto- type met design load
5. Shaft Bend	18,233 in.-lb	23,918 in.-lb	- Catastrophic failure at 130 percent of design load - Test pass

\*Does not include design support tests.

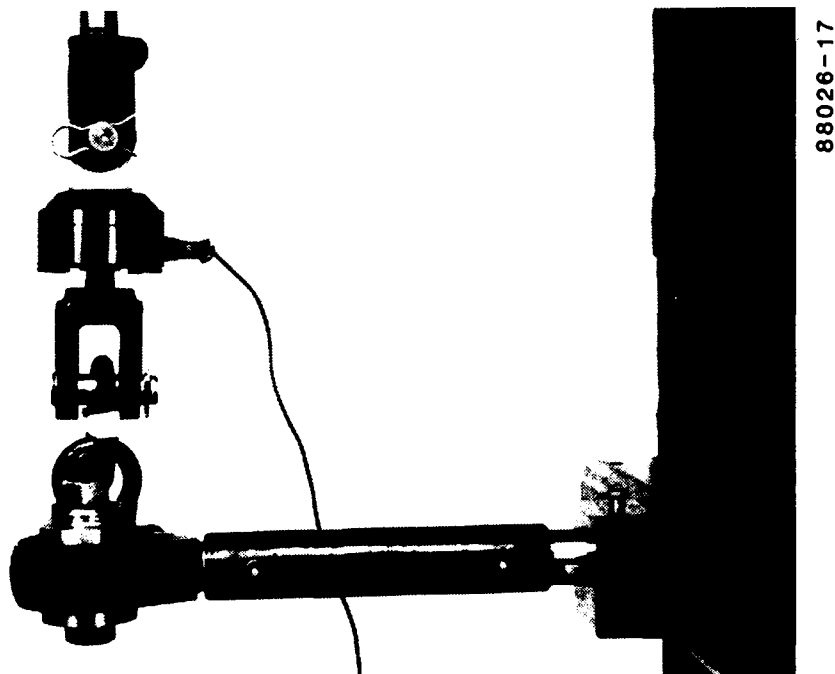


FIGURE 23. POSTTEST VIEW - STATIC TEST, TORSION.

#### 6.3.4 Test 4 - Lateral Bend Test

The graphite shaft was successfully tested beyond its critical moment of 18,708 in.-lb by one percent. The shaft of the knee, however, failed at 55 percent of its critical moment of 6,718 in.-lb. Since the bond was no longer the cause of failure, it was determined that an increase in the diameter of the knee shaft was required. The knee shaft diameter was increased to 1.715 in., as described in Section 5.2.2.2. The knee was also stress relieved after it was machined according to recommendations of the material supplier. A second lateral bend test on the knee was then conducted. The knee successfully sustained the critical load of 6,718 in.-lb. The test was repeated on the same knee to determine repeatability. However, the graphite shaft failed before the knee could reach the critical load. The knee missed its critical load by 13 percent. Nevertheless, the graphite shaft failed at a load 30 percent beyond its critical strength, and the knee demonstrated that it could sustain repeated loads without failure.

#### 6.3.5 Test 5 - Lateral Test of Titanium Neck

This test on the titanium neck demonstrated the design strength of the hip joint assembly. None of the assembly components failed, although slight indentations in the hip joint ball and retaining flange from the force exerted between the two parts were observed. However, one of the bolts used to attach the retaining flange to the test fixture that simulated the pelvis failed. The bolts used in this test were similar in strength to the bolts used on the Hybrid III, which demonstrates that the titanium neck was designed to exceed the design loads of the Hybrid III femur. Figure 24 shows the titanium neck under load.



FIGURE 24. STATIC TESTING, LATERAL BEND TEST OF TITANIUM NECK.

## **7.0 FEASIBILITY ANALYSIS**

### **7.1 FEASIBILITY OF COMPOSITE MATERIALS**

The use of composite materials in structural components has become increasingly popular due to the high strength-to-weight ratio characteristic of composites as compared to metals. Figure 25 compares the tensile strength, tensile modulus, and density of the materials that were used in this program to construct the advanced composite femur. These materials include Ultem 2300 (knee), graphite/epoxy (shaft), and titanium (neck).

Ultem 2300 is similar to both trabecular and cortical bone in strength, modulus, and density, making it an excellent material to represent bone. However, the strength of manikin skeletal components must exceed the strength of bone; therefore Ultem 2300 can be used to fabricate oversized components that are exposed to relatively low forces. Since the knee is exposed to lower bending moments than the rest of the femur, Ultem 2300 was suitable for this application.

Graphite/epoxy is an excellent material for bone design because it exhibits extremely high strength and a density that is similar to bone. In addition to the high strength and low density graphite/epoxy exhibits an elastic modulus that is lower than most metals and therefore close to bone elasticity. This long fiber prepreg was used to laminate the femoral shaft which is exposed to severe loads.

Although not a composite material, titanium has become very popular for use in orthopedic implants because of its strength and low elastic modulus. The latter parameter is an important feature in orthopedics since loads between bone and titanium are more easily transferred than they are between bone and materials with higher moduli. For this program, titanium was selected for its density, which is 55 percent the density of other metals, and for its strength, which is 62 percent higher than that of aluminum bronze. Aluminum bronze is currently used in the Hybrid III hip joint assembly and was replaced in the neck by titanium for added strength.

### **7.2 FEASIBILITY OF COMPOSITE FEMUR**

The feasibility of a composite femur for an anthropomorphic test manikin was determined by the static tests conducted on the prototype femur. Field testing of the femur by the Air Force will further determine its operational suitability. The femur will be tested in a Hybrid III manikin to determine its ease of use, durability, environmental resistance, and dynamic response. Since the composite femur was limited by design to fit the existing Hybrid III manikin, potential improvements to the knee and hip joint assembly exist. The design of a complete skeletal system that includes both the joints and components of an entire leg or skeleton would not be limited by boundary conditions and would be more desirable.

To allow some flexibility in case of failure in the initial development phase, the composite femur was designed with a removable hip joint assembly. This added design constraint could be removed to achieve a lighter, stronger,

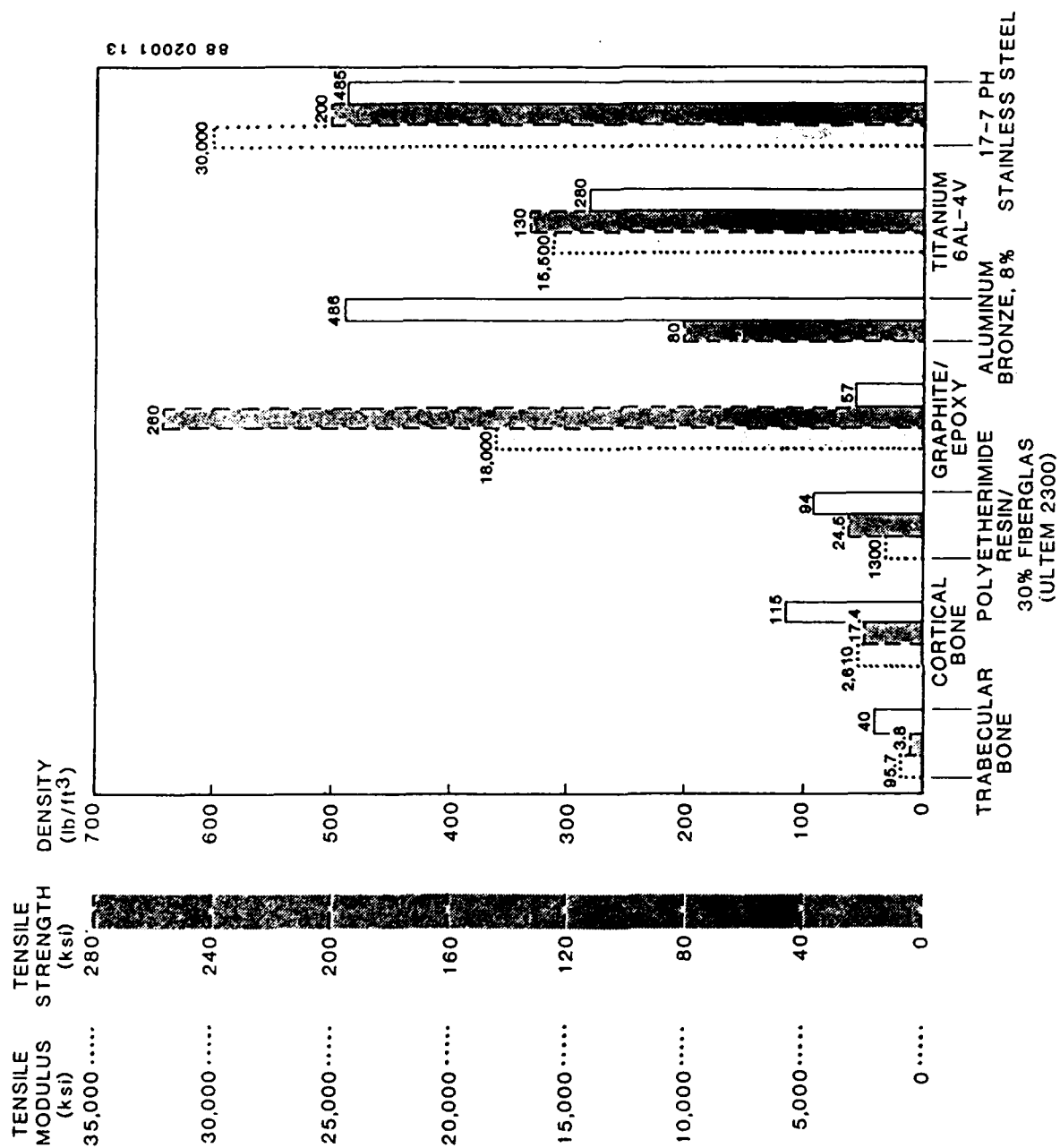


FIGURE 25. COMPARISON OF PROPERTIES FOR MATERIALS USED IN ADVANCED COMPOSITE FEMUR.

and more anatomically designed component. For example, the insert and the fasteners used to provide disassembly could be removed and the design of the knee and hip joint assemblies optimized if the limitations imposed by the Hybrid III configuration were eliminated. Nevertheless, the purpose of this program, to establish the feasibility of using composite materials in anatomical structures that are subjected to severe dynamic loads, was achieved.

The results of the static tests show that composite materials, as applied in the femur, can be effective as structural anatomical components. The weight of the composite femur was reduced, thereby producing a component with biofidelic mass and inertial properties. The mass of the composite femur is 3.9 lb compared to 2.0 lb for the human femur, and the mass moment of inertia for the composite femur is 0.295 in.-lb-sec<sup>2</sup> compared to 0.209 in.-lb-sec<sup>2</sup> for the human femur. This difference in inertial properties is due primarily to the excess weight at the ends of the composite femur resulting from design constraints. Along with the static test results, these features demonstrate that the use of composite materials for a manikin femur is feasible.

### **7.3 FEASIBILITY OF REMAINING SKELETAL COMPONENTS**

The Phase I procedure used to design a feasible composite femur will also be used to design the remaining skeletal components, thereby enhancing the development of a feasible composite skeletal manikin. The candidate skeletal components that would be redesigned with composite materials in Phases II and III include the following:

- Lower limb: pelvis, upper leg, lower leg, foot
- Upper limb: shoulder, upper arm, lower arm, head.

These skeletal components are currently made from metal. Specific emphasis will be made on redesigning the joints of each segment and lowering the mass to achieve biofidelic mass moments of inertia.



## 8.0 CONCLUSIONS

The femur, selected as a representation for all skeletal components, was designed, fabricated, and analyzed, proving that the use of composite materials in manikin skeletal components is feasible.

A significant weight reduction was achieved for the composite femur. The prototype component weighs 3.9 lb compared to the human femur weight of approximately 2.0 lb and the Hybrid III femur weight of 12.5 lb.

It was determined that the inserts and fasteners, which allow disassembly, add unnecessary weight to the femur. If these disassembly components are removed and the disassembly feature eliminated, the total weight of the femur would be reduced by approximately 0.33 lb to 3.57 lb.

The composite femur mass moments of inertia about the transverse axes are 0.295 in.-lb-sec<sup>2</sup> compared to 0.209 in.-lb-sec<sup>2</sup> for the human femur. The moment of inertia for the composite femur is higher than that of the human as a result of some weight concentration at the ends of the femur to accommodate the Hybrid III manikin. The composite femur, however, allows greater mass to be placed in the flesh, resulting in a better approximation of the overall segment mass moments of inertia ( $I_x$ ,  $I_y$  and  $I_z$ ).

The anatomical shape of the composite femur is improved with the increased distance between the shaft axis and ball center.

The strength of the composite femur was tested and shown to significantly exceed that of the Hybrid III and human femurs. Ultimate design loading cases for the tests were based on a calculated design load modified by a dynamic load factor of 2.0 and a safety factor of 1.5. The graphite/epoxy shaft sustained multiple bending loads up to and above the ultimate design load by 30 percent and the thermoplastic knee sustained a load that exceeded the critical load by almost one percent. The titanium neck was designed to exceed the strength of the Hybrid III neck and was tested to the point of failure in the existing Hybrid III attachment hardware.

## 9.0 RECOMMENDATIONS

The following items are recommended to further the development of a more biofidelic test manikin:

- The disassembly feature of the neck/shaft assembly in the composite femur should be eliminated to reduce total weight.
- Dynamic testing of composite skeletal segments should be conducted to determine the strength under high loading rate conditions.
- The anatomical fit of the composite femur with the Hybrid III manikin should be assessed.
- Field testing of the composite femur with the Hybrid III should be conducted to determine the acceptability of the composite material under actual test conditions.
- Further development with composite materials for manikin skeletal components should be continued.
- Joint concepts that reduce mass and maintain articulation range should be emphasized.
- The bulk of segment weight should be distributed in the flesh to provide a more biofidelic mass moment of inertia.
- A search for materials with a specific density of approximately 0.90 is recommended for the flesh.
- The Hybrid III should continue to be used as the baseline for geometry and design; the ADAM should be used as the baseline for joint articulation range of motion.

## 10.0 REFERENCES

1. Foster, J. K., Kortge, J. O., and Wolanin, "Hybrid III-A Biomechanically-Based Crash Test Dummy," paper presented at 21st Stapp Car Crash Conference, Paper No. 770938, Society of Automotive Engineers, Inc., Warrendale, Pennsylvania, 1977.
2. White, R. P., Jr., "ADAM - The Physical Being," paper presented at 25th Annual SAFE Symposium, Las Vegas, Nevada, November 16-20, 1987.
3. Viano, D. C., and Culver, C. C., "Performance of a Shoulder Belt and Knee Restraint in Barrier Crash Simulations," Paper No. 791006, 23rd STAPP Car Crash Conference, October 1979.
4. Frisch, G. D., Whitley, P. E., Wydra, G., et al., "High Speed Ejection Tests of a Modified Hybrid III Manikin," paper presented at 23rd Annual SAFE Symposium, Las Vegas, Nevada, December 1-5, 1985.
5. Military Specification, MIL-S-58095A, General Specification for Seat System: Crash-Resistant, Nonejection, Aircrew.
6. 50th-Percentile Crash Test Dummy Assembly Drawing No. SA150M002, NHTSA, USDOT, Ranges of Motion in Upright Position, March 27, 1973.
7. Tsai, S. W., Composites Design, Ch-11, 3rd Edition, Think Composites, Dayton, Ohio, 1987.
8. Anthropometry and Mass Distribution for Human Analogues, Volume I: Military Male Aviators, Armstrong Aerospace Medical Research Laboratory, Wright-Patterson Air Force Base, Ohio, June 1987.
9. Kaleps, I., and Whitestone, J., "Hybrid III Geometrical and Inertial Properties," 880638, Society of Automotive Engineers, Warrendale, Pennsylvania, 1988.

APPENDIX A  
HUMAN BONE AND FEMUR PROPERTIES

---

TABLE A-1. MECHANICAL PROPERTIES OF HUMAN COMPACT BONE

---

<u>Mechanical Properties</u>	<u>SI Units</u>	<u>English Units</u>
Ultimate Tensile Strength <sup>(1)</sup>	122.6 MPa	17.8 ksi
Ultimate Compressive Strength <sup>(1)</sup>	166.8 MPa	24.2 ksi
Ultimate Bending Strength <sup>(1)</sup>	173.6 MPa	25.2 ksi
Ultimate Torsional Strength <sup>(1)</sup>	57.1 MPa	8.3 ksi
Modulus of Elasticity (Torsion) <sup>(1)</sup>	3,433.5 MPa	498.0 ksi
Modulus of Elasticity (Tension) <sup>(2)</sup>	18,000 MPa	2,611 ksi
Ultimate Percentage Contraction <sup>(1)</sup>	1.9	1.9
Ultimate Percentage Elongation <sup>(1)</sup>	1.44	1.44
Poisson's Ratio <sup>(3)</sup>	0.34	0.34
Density <sup>(4)</sup>	1.80 gm/cm <sup>3</sup>	0.0649 lb/in. <sup>3</sup>

---

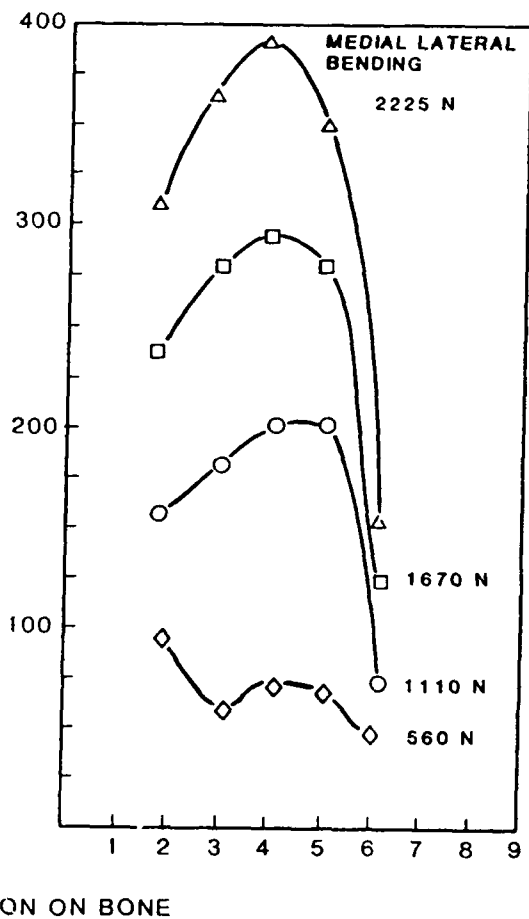
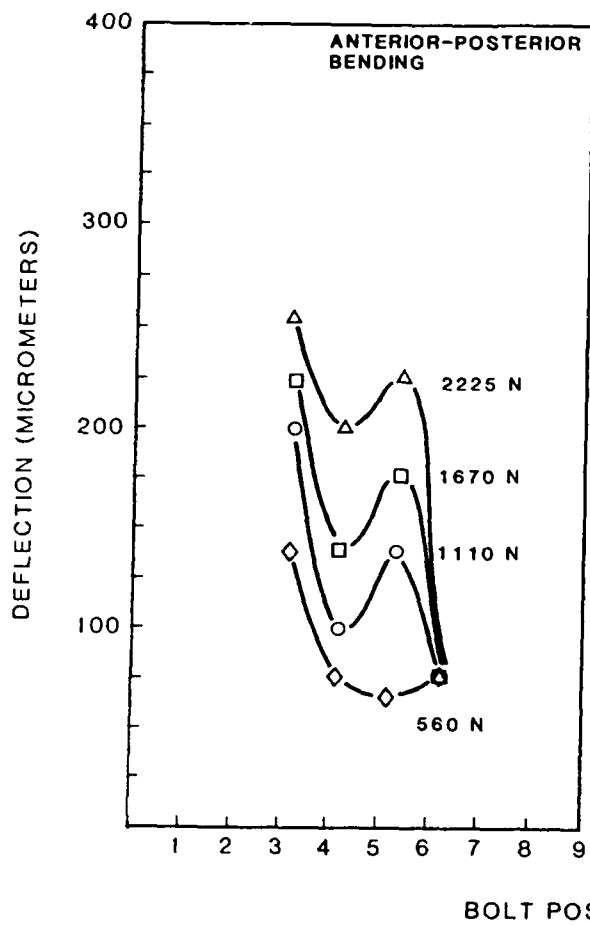
1. Yamada, H., Strength of Biological Materials, edited by F. Gaynor Evans, Ch. 3, The Williams & Wilkins Co., Baltimore, 1970.
  2. McKellop, H., et al., "A Plastic Bone Model for the Evaluation of Femoral Fracture Fixation," Society of Biomaterials Meeting, April 1984.
  3. Van Buskirk, W. C., and Ashman, R. B., "The Elastic Moduli of Bone," Mechanical Properties of Bone, edited by S. Cowen, presented at Joint ASME-ASCE applied Mechanics, Fluid Engineering & Bioengineering Conference, June 1981, AMD-Vol 45, pp. 131-143.
  4. Carter, D. R., and Hayes, W. C., "The Compressive Behavior of Bone as a Two-Phase Porous Structure," Journal of Bone & Joint Surgery, Vol 59-A, No. 7, pp. 954-962, October 1977.
-

TABLE A-2. MECHANICAL PROPERTIES OF HUMAN FEMUR (MIDDLE SECTION OF LONG BONE)<sup>(1)</sup>

<u>Mechanical Properties</u>	<u>SI Units</u>	<u>English Units</u>
Compressive Breaking Load	5,050 kg	11,110 lb
Ultimate Compressive Strength	154 MPa	22.3 ksi
Bending Breaking Load	277 kg	609.4 lb
Ultimate Bending (A-P) Strength	208 MPa	30.2 ksi
Ultimate Deflection (A-P)	12.3 mm	0.48 in.
Ultimate Specific Deflection (A-P)	0.036	0.036
Elastic Modulus	18,345 MPa	2,661 ksi
Modulus of Rigidity	$3,107 \times 10^4$ kg-mm <sup>2</sup>	$10.6 \times 10^4$ lb-in. <sup>2</sup>
Janka's Modulus of Toughness <sup>(2)</sup>	0.07 mm/kg	0.0012 in./lb
Impact Bending Breaking Energy	500 kg-cm	433.1 lb-in.
Impact Bending Strength	1.63 kg-cm/mm <sup>2</sup>	910.8 lb/in.
Torsional Breaking Moment	1,400 kg-cm	1,212.6 lb-in.
Ultimate Torsional Strength	45.3 MPa	6.57 ksi
Ultimate Angle of Twist	1.5°	1.5°

(1) Yamada, H., Strength of Biological Materials, edited by F. Gaynor Evans, Ch. 3, The Williams and Wilkins Co., Baltimore, 1970.

(2) Janka's Modulus of Toughness is the change in deflection divided by bending breaking load.



88 02017 12

a. Bending into and out of the anterior-posterior plane.

b. Bending into and out of the medial-lateral plane.

FIGURE A-1. DEFLECTION AT EACH BOLT POSITION ON EXPERIMENTAL BONE.

**APPENDIX B**  
**CALCULATIONS OF COMPOSITE FEMUR LOADS**



## COMPOSITE FEMUR LOADING CASES

The maximum loads in the femur have been calculated for each of the three principal directions (aircraft coordinate system), based on the dynamic tests specified for crash-resistant crewseats in MIL-S-58095A (Reference 5).

The accelerations shown in Table B-1 were resolved into the three principal directions to obtain the maximum axial, lateral, and vertical components. Therefore, the actual design case is a combination of the axial, lateral, and vertical loads shown.

## DESIGN CONSIDERATIONS

1. Design weights: upper leg = 22 lb  
lower leg and foot = 11 lb
2. Design load factors were obtained from MIL-S-58095A, Table III. A dynamic load factor of 2.0 was applied to the accelerations given in MIL-S-58095A.
3. Design crash loads obtained per item 2 above were increased by a factor of 1.5 to obtain design ultimate loads.
4. Figure B-1 represents the manikin leg geometry used to calculate the design loads.

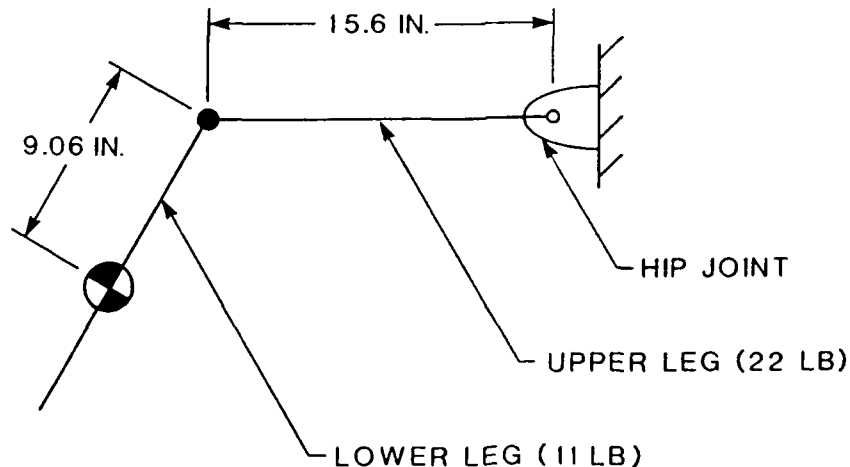
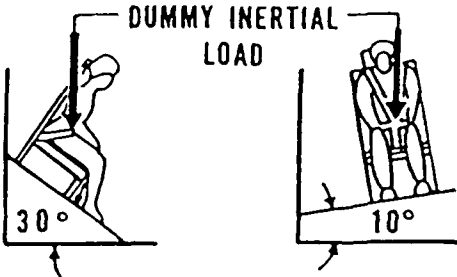
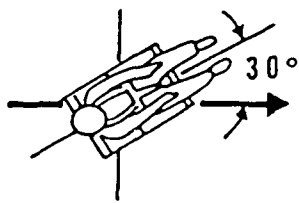
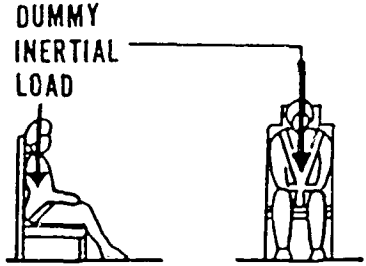


FIGURE B-1. MANIKIN LEG GEOMETRY.

TABLE B-1. MIL-S-58095A DYNAMIC TEST REQUIREMENTS

TEST	CONFIGURATION	PARAMETER	LIMITS
1		$t_1$ SEC $t_2$ SEC G MIN G MAX $\Delta V$ MIN, FT/SEC (M/SEC)	0.043 0.061 46 51 50 (15.2)
2		$t_1$ SEC $t_2$ SEC G MIN G MAX $\Delta V$ MIN, FT/SEC (M/SEC)	0.066 0.100 28 33 50 (15.2)
3 & 4		$t_1$ SEC $t_2$ SEC G MIN G MAX $\Delta V$ MIN, FT/SEC (M/SEC)	0.036 0.051 46 51 42 (12.8)

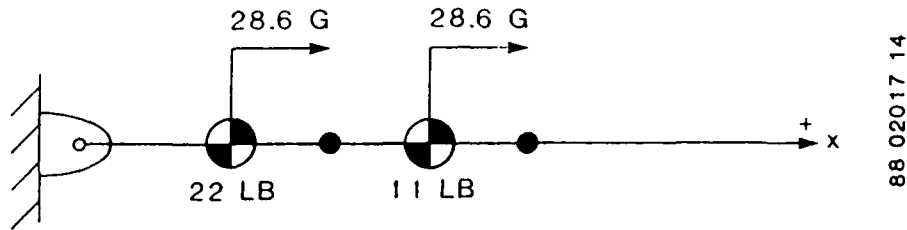
88 02017 02

## LOAD CASES

### 1. CASE 1 - AXIAL LOADING

By inspection, Test 2 (Table B-1) is the critical case.

$$G_x = (33 \text{ G})(\cos 30^\circ) = 28.6 \text{ G}$$

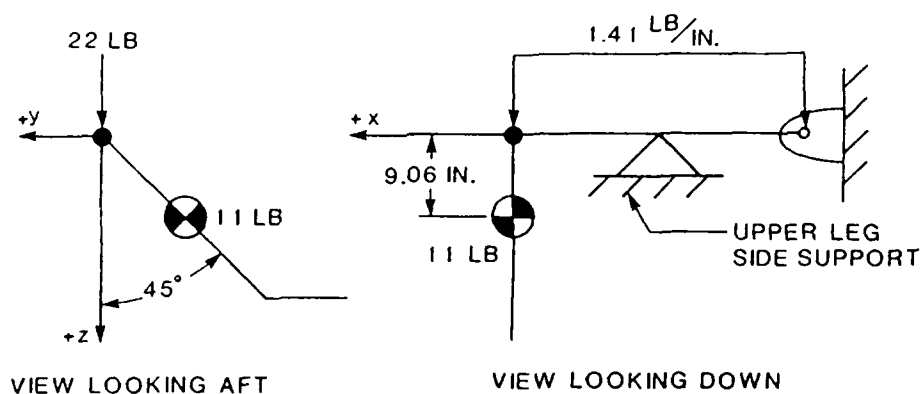


Design axial ultimate load  $F_x = (22 \text{ lb} + 11 \text{ lb})(28.6 \text{ G})(2.0)(1.5)$

$$F_x = 2,831 \text{ lb} (12,592 \text{ N})$$

## 2. CASE 2 - LATERAL LOADING

### Case 2A. Forward-Facing Seat with Side Support for Upper Leg



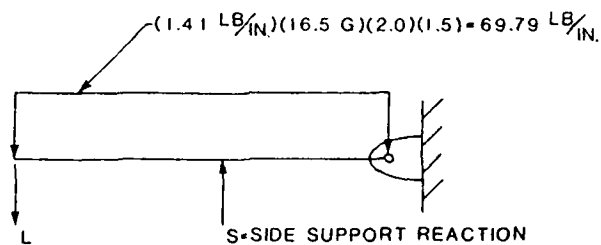
88 02017 13

By inspection, Test 2 (Tabel B-1) is the critical case

$$G_y = (33 \text{ G})(\sin 30^\circ) = 16.5 \text{ G}$$

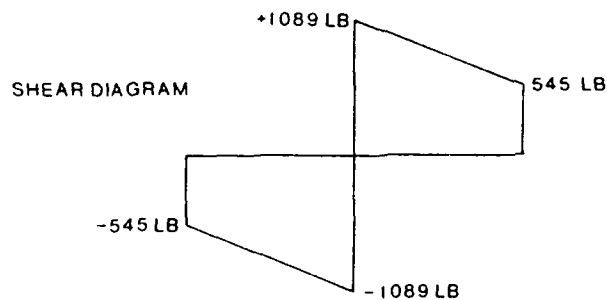
$$\text{Torsion in femur } (M_x) = (11 \text{ lb})(9.06 \text{ in.})(\cos 45^\circ)(2.0)(1.5)(16.5 \text{ G})$$

$$M_x = 3,488 \text{ in.-lb (394 N-m)}$$



88 02017 17

$$L = (11 \text{ LB})(16.5 \text{ G})(2.0)(1.5) = 545 \text{ LB}$$



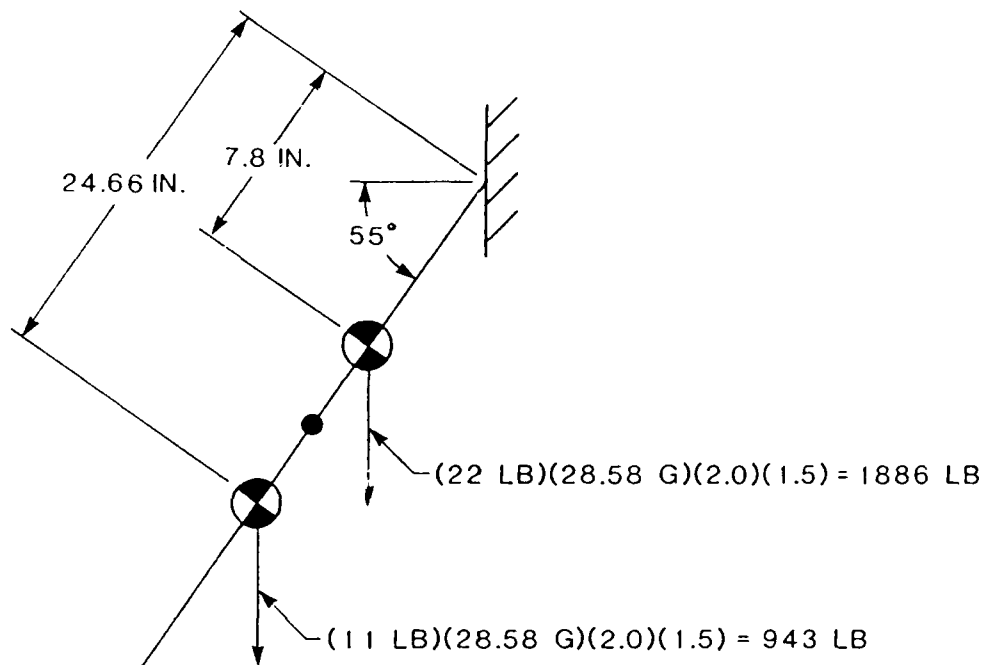
$$\begin{aligned} M_{ys} &= (545 \text{ LB})(7.8 \text{ IN.}) + (69.79 \text{ LB/IN.})(7.8 \text{ IN.})\left(\frac{7.8 \text{ IN.}}{2}\right) \\ &= 6,374 \text{ IN.-LB (720 N-m)} \\ F_z &= 1,089 \text{ LB (4,844 N)} \end{aligned}$$

**Case 2B. Side-Facing Seat with No Side Support for Upper Leg**

The critical load case is Test 2 (Table B-1).

For a side-facing seat:

$$G_y = (33 \text{ G})(\cos 30^\circ) = 28.58 \text{ G}$$



88 02017 16

$$M_z = [(943 \text{ lb})(24.66 \text{ in.}) + (1,886 \text{ lb})(7.8 \text{ in.})]\cos 55^\circ$$

$$= 21,776 \text{ in.-lb (2,460 N-m)}$$

$$F_x = (1,886 \text{ lb} + 943 \text{ lb}) \sin 55^\circ$$

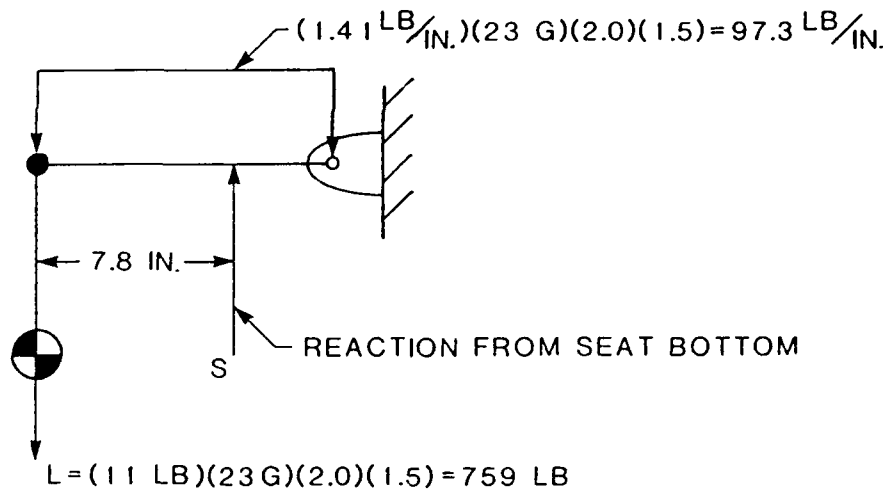
$$= 2,317 \text{ lb (10,308 N)}$$

$$F_y = (1,886 \text{ lb} + 943 \text{ lb})\cos 55^\circ$$

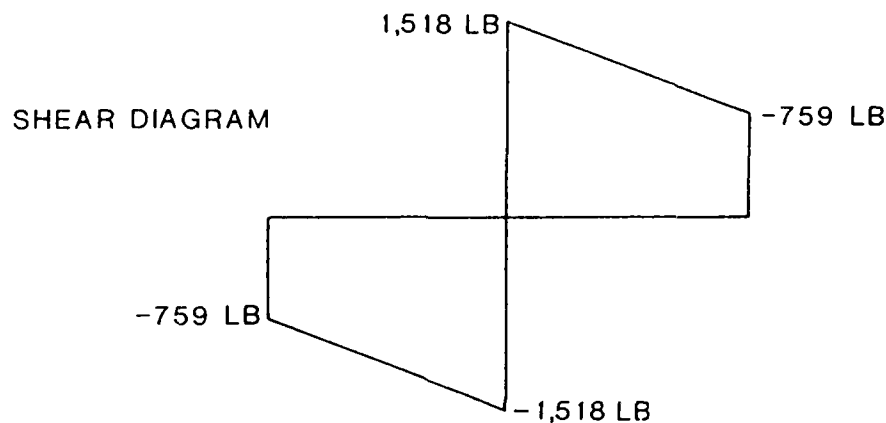
$$= 1,623 \text{ lb (7,218 N)}$$

### 3. CASE 3 - VERTICAL LOADING (EJECTION)

MIL-S-58095A specifies that the vertical deceleration shall not exceed more than 23 G (for .025 sec). Therefore, 23 G will be used as the design limit load factor for the manikin femur. The limit load factor will be increased by a dynamic factor of 2.0 and an ultimate load factor of 1.5.



88 02017 18

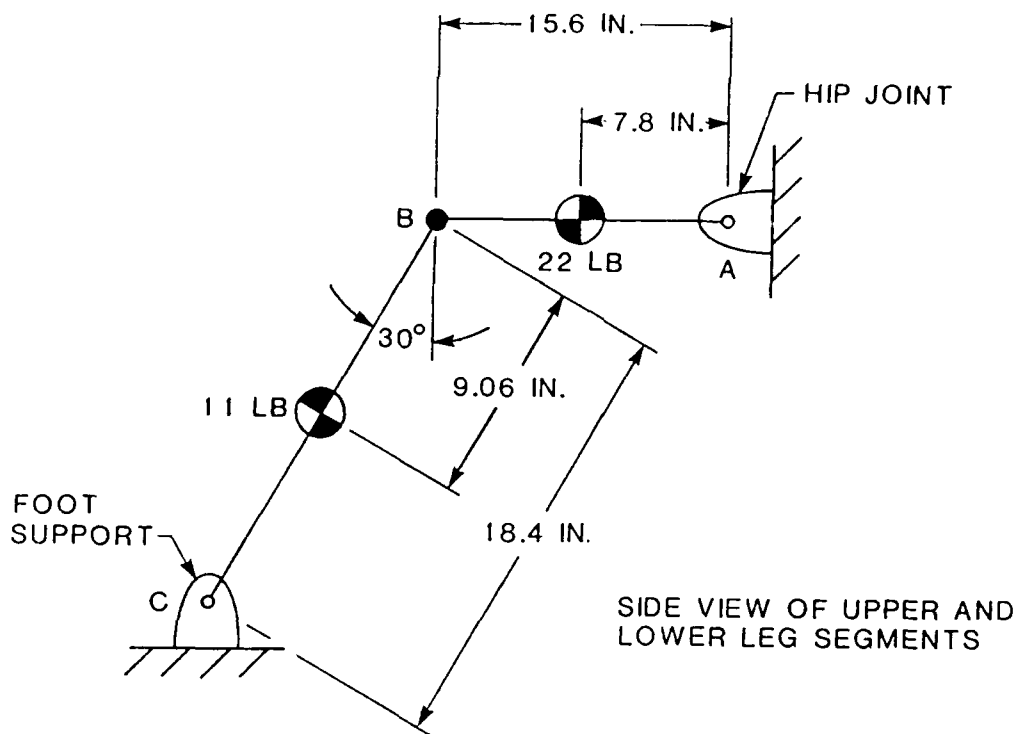


88 02017 20

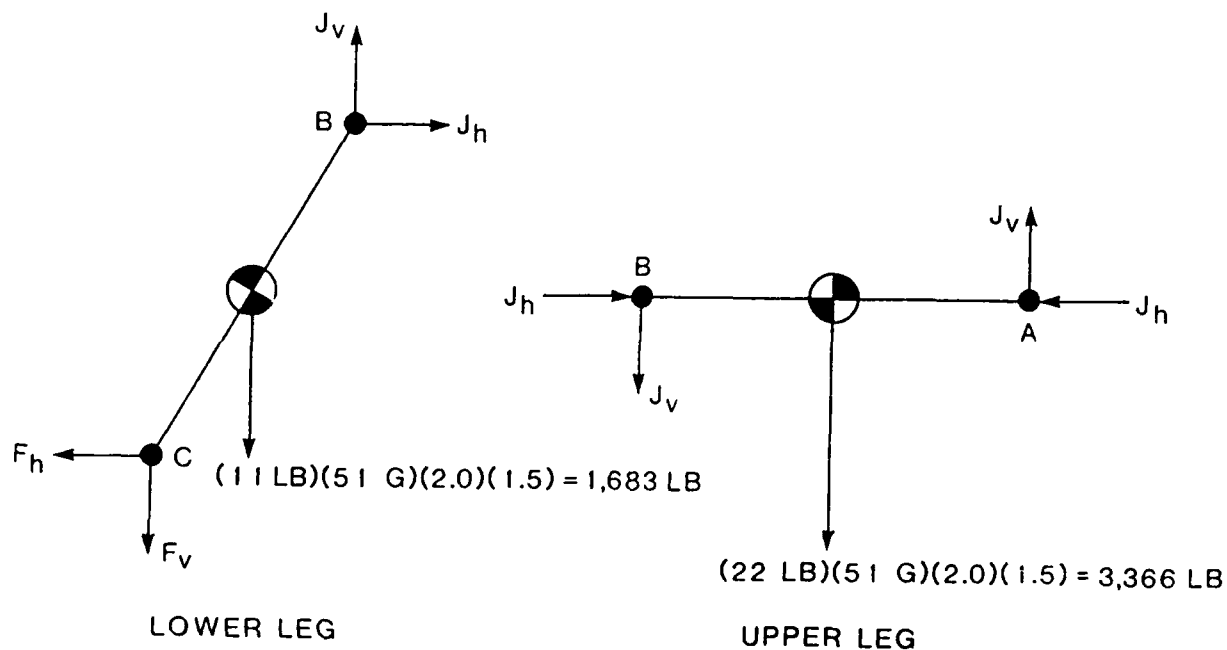
$$\begin{aligned}
 M_{ys} &= (759 \text{ LB})(7.8 \text{ IN.}) + (97.3 \text{ LB/IN.})(7.8 \text{ IN.})\left(\frac{7.8 \text{ IN.}}{2}\right) \\
 &= 8,880 \text{ IN.-LB (1,003 N-m)} \\
 F_z &= 1,518 \text{ LB (6,752 N)}
 \end{aligned}$$

# CASE 4 - VERTICAL DECELERATION (DROP TEST)

Cases 3 and 4 of MIL-S-58095A specify a maximum vertical deceleration of 51 G.



88 02017 19



$$\overset{+}{\curvearrowleft} \sum M_A = 0 = (15.6 \text{ in.})(J_v) + (3,366 \text{ lb})(7.8 \text{ in.})$$

$$J_v = -1,683 \text{ lb}$$

$$\overset{+}{\curvearrowleft} \sum M_c = 0 = (18.4 \text{ in.})(\sin 30^\circ)(J_v) - (18.4 \text{ in.})(\cos 30^\circ)(J_h) - (1,683 \text{ lb})(9.34 \text{ in.})(\sin 30^\circ)$$

$$J_h = \frac{(18.4 \text{ in.})(\sin 30^\circ)(-1,683 \text{ lb}) - (1,683 \text{ lb})(9.34 \text{ in.})(\sin 30^\circ)}{(18.4 \text{ in.})(\cos 30^\circ)}$$

$$J_h = -1,465 \text{ lb}$$

$$F_x = -1,465 \text{ lb} \quad (-6,516 \text{ N})$$

$$F_{z_{\max}} = 1,683 \text{ lb} \quad (7,486 \text{ N})$$

$$\begin{aligned} M_{y_{\max}} &= (1,683 \text{ lb})(7.8 \text{ in.}) \\ &= 13,127 \text{ in.-lb} \quad (1,483 \text{ N-m}) \end{aligned}$$



### CASE 5 - AXIAL KNEE FORCE

The maximum knee loading force taken from the literature is 5,760 lb<sup>(1)</sup>.

With a 1.5 ultimate load factor applied:

$$\begin{aligned} F_x &= (1.5)(5,760 \text{ lb}) \\ &= 8,640 \text{ lb (38,431 N)} \end{aligned}$$

---

(1) Nyquist, G. W. , and King, A. I., Chapter 6, "Lower Extremities," Review of Biomechanical Impact Response and Injury in the Automotive Environment. Phase I Task 8 Report: Advanced Anthropomorphic Test Device Development Program. Edited by Melvin, J. W. and Weber, K., DOT HS 807 042, March 1985.

## **APPENDIX C**

**LAMINATED SHAFT STRAINS, STRESSES,  
AND SAFETY FACTOR FOR THE LOADS  
SHOWN IN FIGURE 6**

## Load Case No 1

Eps1	Eps2	Eps6	k1	k2	k6
.4926E-02	-.5179E-02	.1388E-02	-.2783E-07	.7356E-07	.2431E-07

N1 (LBS)	N2	N6 (LBS)	M1	M2	M6
.8456E+04	.0000E+00	.5570E+03	.0000E+00	.0000E+00	.0000E+00

Temperature difference	.0	Moisture	.0000
------------------------	----	----------	-------

Ply No	Eps-1	Eps-2	Eps-6	Eps-x	Eps-y	Eps-s	*E6
1 Bot	4926.3	-5179.0	1387.9	4926.3	-5179.0	1387.9	
1 Top	4926.3	-5179.0	1387.9	4926.3	-5179.0	1387.9	
2 Bot	4926.3	-5179.0	1387.9	3000.9	-3253.7	-8057.5	
2 Top	4926.3	-5179.0	1387.9	3000.9	-3253.7	-8057.5	
3 Bot	4926.3	-5179.0	1387.9	4926.3	-5179.0	1387.9	
3 Top	4926.3	-5179.0	1387.9	4926.3	-5179.0	1387.9	
4 Bot	4926.3	-5179.0	1387.9	1799.0	-2051.7	9445.4	
4 Top	4926.3	-5179.0	1387.9	1799.0	-2051.7	9445.4	
5 Bot	4926.3	-5179.0	1387.9	4926.3	-5179.0	1387.9	
5 Top	4926.3	-5179.0	1387.9	4926.3	-5179.0	1387.9	
6 Bot	4926.3	-5179.0	1387.9	3000.9	-3253.7	-8057.5	
6 Top	4926.3	-5179.0	1387.9	3000.9	-3253.7	-8057.5	
7 Bot	4926.3	-5179.0	1387.9	4926.3	-5179.0	1387.9	
7 Top	4926.3	-5179.0	1387.9	4926.3	-5179.0	1387.9	
8 Bot	4926.3	-5179.0	1387.9	1799.0	-2051.7	9445.4	
8 Top	4926.3	-5179.0	1387.9	1799.0	-2051.7	9445.4	
9 Bot	4926.3	-5179.0	1387.9	4926.3	-5179.0	1387.9	
9 Top	4926.3	-5179.0	1387.9	4926.3	-5179.0	1387.9	
10 Bot	4926.3	-5179.0	1387.9	3000.9	-3253.7	-8057.5	
10 Top	4926.3	-5179.0	1387.9	3000.9	-3253.7	-8057.5	
11 Bot	4926.3	-5179.0	1387.9	4926.3	-5179.0	1387.9	
11 Top	4926.3	-5179.0	1387.9	4926.3	-5179.0	1387.9	
12 Bot	4926.3	-5179.0	1387.9	4926.3	-5179.0	1387.9	
12 Top	4926.3	-5179.0	1387.9	4926.3	-5179.0	1387.9	
13 Bot	4926.3	-5179.0	1387.9	3000.9	-3253.7	-8057.5	
13 Top	4926.3	-5179.0	1387.9	3000.9	-3253.7	-8057.5	
14 Bot	4926.3	-5179.0	1387.9	4926.3	-5179.0	1387.9	
14 Top	4926.3	-5179.0	1387.9	4926.3	-5179.0	1387.9	
15 Bot	4926.3	-5179.0	1387.9	1799.0	-2051.7	9445.3	
15 Top	4926.3	-5179.0	1387.9	1799.0	-2051.7	9445.3	
16 Bot	4926.3	-5179.0	1387.9	4926.3	-5179.0	1387.9	
16 Top	4926.3	-5179.0	1387.9	4926.3	-5179.0	1387.9	
17 Bot	4926.3	-5179.0	1387.9	3000.9	-3253.7	-8057.5	
17 Top	4926.3	-5179.0	1387.9	3000.9	-3253.7	-8057.5	
18 Bot	4926.3	-5179.0	1387.9	4926.3	-5179.0	1387.9	
18 Top	4926.3	-5179.0	1387.9	4926.3	-5179.0	1387.9	
19 Bot	4926.3	-5179.0	1387.9	1799.0	-2051.7	9445.3	
19 Top	4926.3	-5179.0	1387.9	1799.0	-2051.7	9445.3	

Load Case No 1

20 Bot	4926.3	-5179.0	1387.9	4926.3	-5179.0	1387.9
20 Top	4926.3	-5179.0	1387.9	4926.3	-5179.0	1387.9
21 Bot	4926.3	-5179.0	1387.9	3000.9	-3253.7	-8057.5
21 Top	4926.3	-5179.0	1387.9	3000.9	-3253.7	-8057.5
22 Bot	4926.3	-5179.0	1387.9	4926.3	-5179.0	1387.9
22 Top	4926.3	-5179.0	1387.9	4926.3	-5179.0	1387.9

## Think Composites LPT V3.00

Ply stresses in ksi

Ply No	Sigma-1	Sigma-2	Sigma-6	Sigma-x	Sigma-y	Sigma-s
1 Bot	104.15	-5.21	.92	104.15	-5.21	.92
1 Top	104.15	-5.21	.92	104.15	-5.21	.92
2 Bot	51.33	8.76	26.23	63.41	-3.31	-5.32
2 Top	51.33	8.76	26.23	63.41	-3.31	-5.32
3 Bot	104.15	-5.21	.92	104.15	-5.21	.92
3 Top	104.15	-5.21	.92	104.15	-5.21	.92
4 Bot	33.34	2.50	-14.25	37.97	-2.13	6.23
4 Top	33.34	2.50	-14.25	37.97	-2.13	6.23
5 Bot	104.15	-5.21	.92	104.15	-5.21	.92
5 Top	104.15	-5.21	.92	104.15	-5.21	.92
6 Bot	51.33	8.76	26.23	63.41	-3.31	-5.32
6 Top	51.33	8.76	26.23	63.41	-3.31	-5.32
7 Bot	104.15	-5.21	.92	104.15	-5.21	.92
7 Top	104.15	-5.21	.92	104.15	-5.21	.92
8 Bot	33.34	2.50	-14.25	37.97	-2.13	6.23
8 Top	33.34	2.50	-14.25	37.97	-2.13	6.23
9 Bot	104.15	-5.21	.92	104.15	-5.21	.92
9 Top	104.15	-5.21	.92	104.15	-5.21	.92
10 Bot	51.33	8.76	26.23	63.41	-3.31	-5.32
10 Top	51.33	8.76	26.23	63.41	-3.31	-5.32
11 Bot	104.15	-5.21	.92	104.15	-5.21	.92
11 Top	104.15	-5.21	.92	104.15	-5.21	.92
12 Bot	104.15	-5.21	.92	104.15	-5.21	.92
12 Top	104.15	-5.21	.92	104.15	-5.21	.92
13 Bot	51.33	8.76	26.23	63.41	-3.31	-5.32
13 Top	51.33	8.76	26.23	63.41	-3.31	-5.32
14 Bot	104.15	-5.21	.92	104.15	-5.21	.92
14 Top	104.15	-5.21	.92	104.15	-5.21	.92
15 Bot	33.34	2.50	-14.25	37.97	-2.13	6.23
15 Top	33.34	2.50	-14.25	37.97	-2.13	6.23
16 Bot	104.15	-5.21	.92	104.15	-5.21	.92
16 Top	104.15	-5.21	.92	104.15	-5.21	.92
17 Bot	51.33	8.76	26.23	63.41	-3.31	-5.32
17 Top	51.33	8.76	26.23	63.41	-3.31	-5.32
18 Bot	104.15	-5.21	.92	104.15	-5.21	.92
18 Top	104.15	-5.21	.92	104.15	-5.21	.92
19 Bot	33.34	2.50	-14.25	37.97	-2.13	6.23
19 Top	33.34	2.50	-14.25	37.97	-2.13	6.23
20 Bot	104.15	-5.21	.92	104.15	-5.21	.92
20 Top	104.15	-5.21	.92	104.15	-5.21	.92
21 Bot	51.33	8.76	26.23	63.41	-3.31	-5.32
21 Top	51.33	8.76	26.23	63.41	-3.31	-5.32
22 Bot	104.15	-5.21	.92	104.15	-5.21	.92
22 Top	104.15	-5.21	.92	104.15	-5.21	.92

Load Case No 1

Think Composites LPT V3.00

Ply No	Angle	Matr No	z-bottom	z-top	R-bottom	R-top
1	.0	15	-.055000	-.050000	1.94	1.94
2	30.0	15	-.050000	-.045000	1.63	1.63
3	.0	15	-.045000	-.040000	1.94	1.94
4	-30.0	15	-.040000	-.035000	1.48	1.48
5	.0	15	-.035000	-.030000	1.94	1.94
6	30.0	15	-.030000	-.025000	1.63	1.63
7	.0	15	-.025000	-.020000	1.94	1.94
8	-30.0	15	-.020000	-.015000	1.48	1.48
9	.0	15	-.015000	-.010000	1.94	1.94
10	30.0	15	-.010000	-.005000	1.63	1.63
11	.0	15	-.005000	.000000	1.94	1.94
12	.0	15	.000000	.005000	1.94	1.94
13	30.0	15	.005000	.010000	1.63	1.63
14	.0	15	.010000	.015000	1.94	1.94
15	-30.0	15	.015000	.020000	1.48	1.48
16	.0	15	.020000	.025000	1.94	1.94
17	30.0	15	.025000	.030000	1.63	1.63
18	.0	15	.030000	.035000	1.94	1.94
19	-30.0	15	.035000	.040000	1.48	1.48
20	.0	15	.040000	.045000	1.94	1.94
21	30.0	15	.045000	.050000	1.63	1.63
22	.0	15	.050000	.055000	1.94	1.94

MARGIN OF SAFETY (M.S.) = R-1

## Load Case No 2

Think Composites LPT V3.00

Eps1	Eps2	Eps6	k1	k2	k6
.5034E-02	-.4845E-02	-.3029E-02	-.2808E-07	.7468E-07	-.1428E-07

N1 (LB)	N2	N6 (LB)	M1	M2	M6
.8456E+04	.0000E+00	-.5570E+03	.0000E+00	.0000E+00	.0000E+00

Temperature difference	.0	Moisture	.0000
------------------------	----	----------	-------

Ply No	Eps-1	Eps-2	Eps-6	Eps-x	Eps-y	Eps-s	*E6
1 Bot	5034.4	-4845.1	-3029.0	5034.4	-4845.1	-3029.0	
1 Top	5034.4	-4845.0	-3029.0	5034.4	-4845.0	-3029.0	
2 Bot	5034.4	-4845.0	-3029.0	1252.9	-1063.6	-10070.3	
2 Top	5034.4	-4845.0	-3029.0	1252.9	-1063.6	-10070.3	
3 Bot	5034.4	-4845.0	-3029.0	5034.4	-4845.0	-3029.0	
3 Top	5034.4	-4845.0	-3029.0	5034.4	-4845.0	-3029.0	
4 Bot	5034.4	-4845.0	-3029.0	3876.1	-3686.8	7041.3	
4 Top	5034.4	-4845.0	-3029.0	3876.1	-3686.8	7041.3	
5 Bot	5034.4	-4845.0	-3029.0	5034.4	-4845.0	-3029.0	
5 Top	5034.4	-4845.0	-3029.0	5034.4	-4845.0	-3029.0	
6 Bot	5034.4	-4845.0	-3029.0	1252.9	-1063.6	-10070.3	
6 Top	5034.4	-4845.0	-3029.0	1252.9	-1063.6	-10070.3	
7 Bot	5034.4	-4845.0	-3029.0	5034.4	-4845.0	-3029.0	
7 Top	5034.4	-4845.0	-3029.0	5034.4	-4845.0	-3029.0	
8 Bot	5034.4	-4845.0	-3029.0	3876.1	-3686.8	7041.3	
8 Top	5034.4	-4845.0	-3029.0	3876.1	-3686.8	7041.3	
9 Bot	5034.4	-4845.0	-3029.0	5034.4	-4845.0	-3029.0	
9 Top	5034.4	-4845.0	-3029.0	5034.4	-4845.0	-3029.0	
10 Bot	5034.4	-4845.0	-3029.0	1252.9	-1063.6	-10070.3	
10 Top	5034.4	-4845.0	-3029.0	1252.9	-1063.6	-10070.3	
11 Bot	5034.4	-4845.0	-3029.0	5034.4	-4845.0	-3029.0	
11 Top	5034.4	-4845.0	-3029.0	5034.4	-4845.0	-3029.0	
12 Bot	5034.4	-4845.0	-3029.0	5034.4	-4845.0	-3029.0	
12 Top	5034.4	-4845.0	-3029.0	5034.4	-4845.0	-3029.0	
13 Bot	5034.4	-4845.0	-3029.0	1252.9	-1063.6	-10070.3	
13 Top	5034.4	-4845.0	-3029.0	1252.9	-1063.6	-10070.3	
14 Bot	5034.4	-4845.0	-3029.0	5034.4	-4845.0	-3029.0	
14 Top	5034.4	-4845.0	-3029.0	5034.4	-4845.0	-3029.0	
15 Bot	5034.4	-4845.0	-3029.0	3876.1	-3686.8	7041.3	
15 Top	5034.4	-4845.0	-3029.0	3876.1	-3686.8	7041.3	
16 Bot	5034.4	-4845.0	-3029.0	5034.4	-4845.0	-3029.0	
16 Top	5034.4	-4845.0	-3029.0	5034.4	-4845.0	-3029.0	
17 Bot	5034.4	-4845.0	-3029.0	1252.9	-1063.6	-10070.3	
17 Top	5034.4	-4845.0	-3029.0	1252.9	-1063.6	-10070.3	
18 Bot	5034.4	-4845.0	-3029.0	5034.4	-4845.0	-3029.0	
18 Top	5034.4	-4845.0	-3029.0	5034.4	-4845.0	-3029.0	
19 Bot	5034.4	-4845.0	-3029.0	3876.1	-3686.8	7041.3	
19 Top	5034.4	-4845.0	-3029.0	3876.1	-3686.8	7041.3	

Load Case No 2

Think Composites LPT V3.00

20 Bot	5034.4	-4845.0	-3029.0	5034.4	-4845.0	-3029.0
20 Top	5034.4	-4845.0	-3029.0	5034.4	-4845.0	-3029.0
21 Bot	5034.4	-4845.0	-3029.0	1252.9	-1063.6	-10070.3
21 Top	5034.4	-4845.0	-3029.0	1252.9	-1063.6	-10070.3
22 Bot	5034.4	-4845.0	-3029.0	5034.4	-4845.0	-3029.0
22 Top	5034.4	-4845.0	-3029.0	5034.4	-4845.0	-3029.0



## Think Composites LPT V3.00

Ply stresses in ksi

Ply No	Sigma-1	Sigma-2	Sigma-6	Sigma-x	Sigma-y	Sigma-s
1 Bot	106.63	-4.70	-2.00	106.63	-4.70	-2.00
1 Top	106.63	-4.70	-2.00	106.63	-4.70	-2.00
2 Bot	25.46	.17	8.61	26.60	-.97	-6.65
2 Top	25.46	.17	8.61	26.60	-.97	-6.65
3 Bot	106.63	-4.70	-2.00	106.63	-4.70	-2.00
3 Top	106.63	-4.70	-2.00	106.63	-4.70	-2.00
4 Bot	64.72	13.84	-34.77	82.11	-3.55	4.65
4 Top	64.72	13.84	-34.77	82.11	-3.55	4.65
5 Bot	106.63	-4.70	-2.00	106.63	-4.70	-2.00
5 Top	106.63	-4.70	-2.00	106.63	-4.70	-2.00
6 Bot	25.46	.17	8.61	26.60	-.97	-6.65
6 Top	25.46	.17	8.61	26.60	-.97	-6.65
7 Bot	106.63	4.70	-2.00	106.63	-4.70	-2.00
7 Top	106.63	-4.70	-2.00	106.63	-4.70	-2.00
8 Bot	64.72	13.84	-34.77	82.11	-3.55	4.65
8 Top	64.72	13.84	-34.77	82.11	-3.55	4.65
9 Bot	106.63	-4.70	-2.00	106.63	-4.70	-2.00
9 Top	106.63	-4.70	-2.00	106.63	-4.70	-2.00
10 Bot	25.46	.17	8.61	26.60	-.97	-6.65
10 Top	25.46	.17	8.61	26.60	-.97	-6.65
11 Bot	106.63	-4.70	-2.00	106.63	-4.70	-2.00
11 Top	106.63	-4.70	-2.00	106.63	-4.70	-2.00
12 Bot	106.63	-4.70	-2.00	106.63	-4.70	-2.00
12 Top	106.63	-4.70	-2.00	106.63	-4.70	-2.00
13 Bot	25.46	.17	8.61	26.60	-.97	-6.65
13 Top	25.46	.17	8.61	26.60	-.97	-6.65
14 Bot	106.63	-4.70	-2.00	106.63	-4.70	-2.00
14 Top	106.63	-4.70	-2.00	106.63	-4.70	-2.00
15 Bot	64.72	13.84	-34.77	82.11	-3.55	4.65
15 Top	64.72	13.84	-34.77	82.11	-3.55	4.65
16 Bot	106.63	-4.70	-2.00	106.63	-4.70	-2.00
16 Top	106.63	-4.70	-2.00	106.63	-4.70	-2.00
17 Bot	25.46	.17	8.61	26.60	-.97	-6.65
17 Top	25.46	.17	8.61	26.60	-.97	-6.65
18 Bot	106.63	-4.70	-2.00	106.63	-4.70	-2.00
18 Top	106.63	-4.70	-2.00	106.63	-4.70	-2.00
19 Bot	64.72	13.84	-34.77	82.11	-3.55	4.65
19 Top	64.72	13.84	-34.77	82.11	-3.55	4.65
20 Bot	106.63	-4.70	-2.00	106.63	-4.70	-2.00
20 Top	106.63	-4.70	-2.00	106.63	-4.70	-2.00
21 Bot	25.46	.17	8.61	26.60	-.97	-6.65
21 Top	25.46	.17	8.61	26.60	-.97	-6.65
22 Bot	106.63	-4.70	-2.00	106.63	-4.70	-2.00
22 Top	106.63	-4.70	-2.00	106.63	-4.70	-2.00

Load Case No 2

Think Composites LPT V3.00

Ply No	Angle	Matr No	z-bottom	z-top	R-bottom	R-top
1	.0	15	-.055000	-.050000	1.86	1.86
2	30.0	15	-.050000	-.045000	1.36	1.36
3	.0	15	-.045000	-.040000	1.86	1.86
4	-30.0	15	-.040000	-.035000	1.66	1.66
5	.0	15	-.035000	-.030000	1.86	1.86
6	30.0	15	-.030000	-.025000	1.36	1.36
7	.0	15	-.025000	-.020000	1.86	1.86
8	-30.0	15	-.020000	-.015000	1.66	1.66
9	.0	15	-.015000	-.010000	1.86	1.86
10	30.0	15	-.010000	-.005000	1.36	1.36
11	.0	15	-.005000	.000000	1.86	1.86
12	.0	15	.000000	.005000	1.86	1.86
13	30.0	15	.005000	.010000	1.36	1.36
14	.0	15	.010000	.015000	1.86	1.86
15	-30.0	15	.015000	.020000	1.66	1.66
16	.0	15	.020000	.025000	1.86	1.86
17	30.0	15	.025000	.030000	1.36	1.36
18	.0	15	.030000	.035000	1.86	1.86
19	-30.0	15	.035000	.040000	1.66	1.66
20	.0	15	.040000	.045000	1.86	1.86
21	30.0	15	.045000	.050000	1.36	1.36

MARGIN OF SAFETY (M.S.) = R - 1

APPENDIX D  
CALCULATION OF STRESS IN  
THE KNEE FITTING

Using the schematic shown in Figure D-1, the critical moment  $M_A$  and the critical stress  $F_A$  in the composite knee fitting were calculated as follows:

$$M_A = (943 \text{ lb})(\cos 55^\circ)(9.06 \text{ in.} + 3.36 \text{ in.}) = 6,718 \text{ in.-lb}$$

$$F_A = \frac{P}{A} + \frac{M_C}{I} = \frac{(943 \text{ lb})(\sin 55^\circ)}{\pi(0.86 \text{ in.})^2} + \frac{(32)(6,718 \text{ in.-lb})}{\pi(1.715 \text{ in.})^3} = 13,900 \text{ psi}$$

The stress margin of safety is:

$$M.S. = \frac{F_{ty}}{13,900 \text{ psi}} - 1 = \frac{24,500}{13,900 \text{ psi}} - 1 = +.7626$$

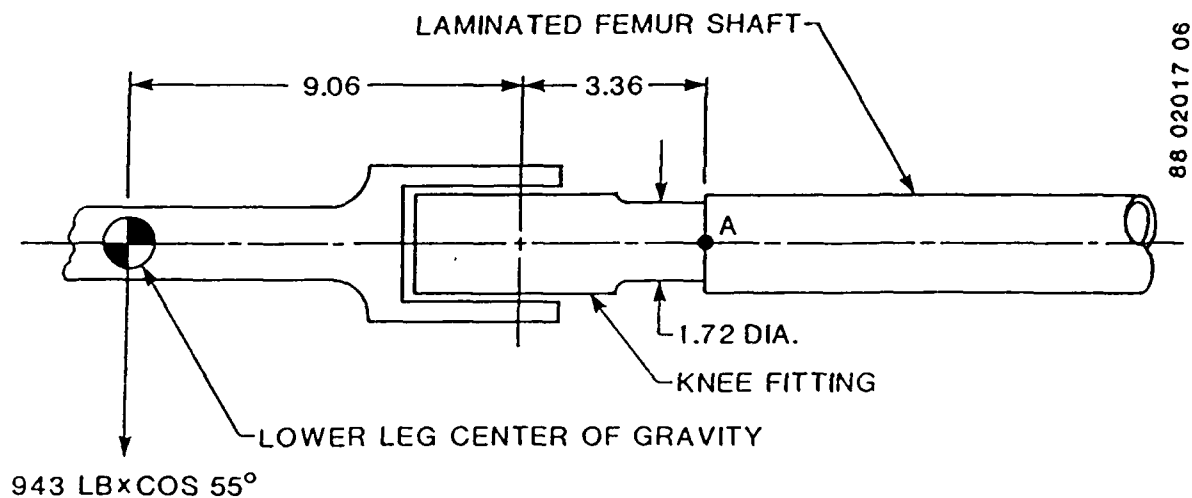


FIGURE D-1. CRITICAL LOADING OF ADVANCED COMPOSITE KNEE JOINT FITTING.

APPENDIX E

CALCULATION OF ULTIMATE STRENGTH OF  
YELLOW BRASS NECK  
OF EXISTING HYBRID III FEMUR

To determine the minimum design strength for the composite hip joint neck, the ultimate strength in the Hybrid III femoral neck was calculated. The moment required to fail the Hybrid III neck shaft (Figure E-1) was calculated as follows:

Bending Modulus of Rupture:

$$F_{bu} = F_{tu} + (.7)F_{ty}$$

$$F_{bu} = 177,100 \text{ psi}$$

Since,

$$F_{bu} = \frac{32 M}{\pi D^3} = \frac{(32)(M)}{\pi (.75)^3} = 177,100 \text{ psi}$$

$$M = 7,335 \text{ in.-lb (moment required to fail the shaft)}$$

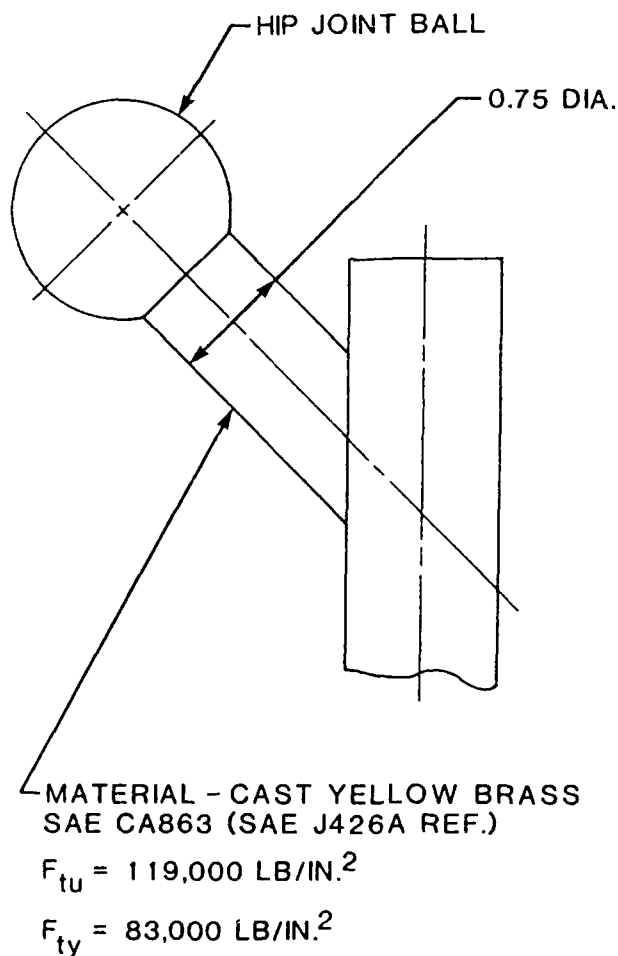


FIGURE E-1. HYBRID III HIP JOINT ASSEMBLY.